A Circuit Model BOSS Simulation of Nonlinear Effects in Long Distance Fiber Optic Systems
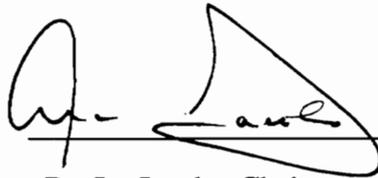
by

Shilpa D. Mehta

Thesis submitted to the Faculty of the

Virginia Polytechnic Institute and State University

in partial fulfillment of the requirements for the degree of

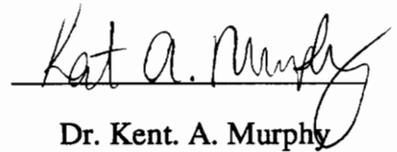**Master of Science**

in

Electrical Engineering

APPROVED:

Dr. Ira Jacobs, Chairman

Dr. Richard. O. Claus

Dr. Kent. A. Murphy

July, 1993

Blacksburg, Virginia

A Circuit Model BOSS Simulation of Nonlinear Effects in Long Distance Fiber Optic Systems

Shilpa D. Mehta

Fiber & Electro-Optic Research Center

Bradley Department of Electrical Engineering

Virginia Polytechnic Institute and State University

Blacksburg, VA 24061-0111

The combined effect of group velocity dispersion (GVD) and nonlinearity limits the transmission distance of fiber optic communication systems. By designing a circuit that can model this effect and simulating it using the Block Oriented Systems Simulator (BOSS), we can study the pulse distortion and broadening that may occur. The nonlinearity considered here is self-phase modulation (SPM). A loop system is designed where each pass of the system corresponds to 200 km of fiber. The system mainly consists of a Butterworth bandpass filter which models the dispersion in the fiber and a VCO that imposes a phase modulation on the input signal thus modeling the intensity dependent phase shift due to SPM. By changing various parameters of the circuit, the dispersion limited distance, the nonlinearity limited distance and other related factors can be altered. With D=-0.04 ps/km.nm, the effect of changing the nonlinear limited distance and thus the nonlinear effect is studied and simulated. The results are compared with a simple theoretical model for pulse broadening that has appeared in the literature. Although the

Abstract

simulation results exhibit the same qualitative behavior as the theory, there are significant quantitative differences. The reason for these differences are discussed.

Abstract

Acknowledgments

I would like to thank my advisor, Dr. Ira Jacobs, for encouraging and guiding me through this thesis. The knowledge and insight that he has in the field of communications and fiber optics is remarkable. Having him as both a teacher and an advisor has been a truly rewarding experience. I would also like to thank my committee members Dr. Richard. O. Claus and Dr. Kent. A. Murphy for their support and valuable suggestions.

I am grateful to all the members of FEORC for introducing me to various aspects of fiber optics and making my learning experience a pleasure. I also want to thank Dr. Ken Baker for helping me to learn BOSS.

Finally, I would like to thank my parents, Dilip and Ranjan Mehta, for being my source of inspiration and my fiancé, Ketan Kamdar, for his continuous support and encouragement.

Table of Contents

List of Figures

List of Tables

Chapter 1: Introduction

1.1 Background

Lightwave systems have played a tremendous role in the advancement of communication technology. Fiber, having a large bandwidth, has been used as a medium to transport data, for example, between telephone switching offices on the same continent and even overseas. Efforts are now being directed to extending this fiber from the switch to the end-user. Long distance fiber systems can carry higher data rates over greater repeater distances than any other transmission medium currently proposed. In the past decade the product of bit-rate and transmission distance for a single wavelength channel has shown a growth rate of roughly a factor of two per year [1]. In a recent test it was shown that light pulses transmitted at a rate of 10 Gb/s over a distance of 2000 km showed a BER lower than 1 in 10^{13} [2]. The advent of Erbium doped fiber amplifiers and solitons has given more room for improvement.

With the increase in bit rate, dispersive effects in fiber have become more important. Due to dispersion, the data pulses spread out and overlap with successive pulses causing an

increase in BER. Higher bit rates give rise to a smaller bit period T. Thus even a small increase in pulse width is of significant concern, especially for long distance links. The use of linear (non-regenerative) repeaters in long distance links causes an accumulation of dispersion and in this case too, a small dispersion will cause a large amount of pulse broadening. The effect of nonlinearity has also become of more concern due to these reasons. Thus not only are dispersion and attenuation limiting factors in fiber optic links but nonlinear properties of fiber have also become an operating limitation.

1.2 Effect of different types of nonlinearities

A linear medium is characterized by a propagation constant Γ. It is given by

$$\Gamma = \alpha + j\beta, \tag{1.1}$$

where α is the attenuation and β is the phase constant. In a weakly nonlinear medium α and β are functions of the signal intensity and this may result in distortion, enhanced attenuation and intermodulation of optical signals. Nonlinear systems may be classified on the basis of whether the nonlinearity affects primarily the amplitude or the phase of the signal. A brief outline of the types of nonlinearities in fiber, belonging to these two classes, is given as follows.

(1) Stimulated Scattering

Stimulated scattering causes a variation in amplitude and distortion of the input signal. The two main types of nonlinearities due to stimulated scattering are:

• Stimulated Raman Scattering (SRS)

SRS is caused by the interaction between the silica molecules of the fiber and light. This interaction causes frequency conversion of light which leads to the generation of interfering signals in a multi-channel system [3]. SRS introduces cross-coupling between adjacent channels and thus limits the number of channels and the maximum channel spacing in a Wavelength Division Multiplexed (WDM) system.

• Stimulated Brillouin Scattering (SBS)

SBS is similar to SRS except that frequency conversion occurs due to interaction of light and sound waves in a fiber. Backscattering is the prime effect of SBS. In the forward direction it tends to increase Relative Intensity Noise (RIN) and thus degrades analog systems.

(2) Nonlinear index (Kerr effect)

At high intensities of light, the refractive index (RI) of the fiber increases with an increase in intensity. This phenomenon is known as the Kerr effect. As a result of the intensity dependence of the RI, the change in RI tends to modulate the phase of the propagating wave. This effect will be significant in angle modulated systems. It will degrade systems

in which the receiver is sensitive to changes in the carrier phase angle (coherent homodyne or heterodyne detection) [3]. It will also affect direct detection systems owing to mechanisms such as dispersion that converts phase fluctuations to intensity fluctuations. Depending on the number of inputs to the system, the main types of this nonlinearity are:

• Self Phase Modulation (SPM)

SPM involves a single input, and will be studied in detail in this thesis. The SPM induced phase change is a function of time and causes an increase in spectral width. With dispersion, the input pulse broadens and distorts. This is the primary effect that will be studied. A more detailed explanation of SPM is given in section 2.2.2.

• Cross Phase Modulation (XPM)

XPM is similar to SPM but in this case there are two input signals at different wavelengths. A phase shift is induced in one of the signals due to the other co-propagating signal.

• Intermodulation (Four-photon mixing)

Intermodulation occurs when two or more signals combine to create new signals at the sum and difference frequencies.

The propagation of a pulse depends on the relationship between the length of the fiber (L), the dispersion limiting distance (L_d) and the nonlinearity limiting distance (L_{nl}). L_d is the distance at which the increase in pulse width becomes comparable to the original pulse width. L_{nl} is the distance at which the pulse distortion produced becomes prominent. A

more precise definition of these terms will be given in section 2.2. When $L<<L_d$ and $L<<L_{nl}$, the dispersive and nonlinear effects are not significant. In this case, the pulse will maintain its shape during propagation. When $L>L_d$ but $L<<L_{nl}$, dispersion plays a significant role, but nonlinearity may be neglected, which is the case in most of the present fiber optic systems. When $L<<L_d$ but $L>L_{nl}$, the effect of nonlinearity is prominent as compared to dispersion and SPM will cause spectral broadening and distortion. Group velocity dispersion or GVD (explained in section 2.2.1) causes temporal spreading of the pulse. The case that is of interest to us is when the ratio of L_d to L_{nl} is much greater than one, i.e. when the effect of nonlinearity is prominent. The combined effect of self-phase modulation and group velocity dispersion in this regime is studied.

1.3 Overview

The aim of this thesis is to design and simulate an electrical circuit that can model a nonlinear, dispersive long distance link. The combined effects of the Kerr nonlinearity and GVD will be studied. The Block Oriented Systems Simulator (BOSS) will be used as the simulation tool. Parameters such as power, coefficient of dispersion, length of the link etc. can be varied and the dependence of these parameters will be studied. From the results of the simulation we can observe the distortion and dispersion of the input pulse at various distances without having to design an experimental setup. Chapter 2 gives a detailed explanation of GVD and SPM. Chapter 3 outlines the circuit design and difficulties encountered. In Chapter 4, the various simulations carried out and the results obtained are discussed. Conclusions are summarized in Chapter 5.

Chapter 2: Dispersion and Self Phase Modulation

2.1 Propagation equations

To understand the facets of GVD and SPM, a brief analytical explanation of the propagation of a pulse in a single mode fiber is given. All the equations in this chapter have been taken from [4] and one can refer to it for more details. It is assumed that the field intensity, may be expressed in terms of a slowly varying envelope function $A(z,t)$ multiplying a high frequency carrier term $e^{i[\beta(\omega)z - \omega t]}$. Expanding the phase, $\beta(\omega)$, in a power series around the center frequency ω_0, neglecting higher than second order terms, and substituting into the wave equation gives the following nonlinear partial differential equation for $A(z,t)$

$$\frac{\partial A}{\partial z} + \beta_1 \frac{\partial A}{\partial t} + \frac{i}{2}\beta_2 \frac{\partial^2 A}{\partial t^2} + \frac{\alpha}{2} A = i\gamma |A|^2 A \ , \tag{2.1}$$

where α is the power attenuation constant, γ is the nonlinearity constant.

$$\beta_1 = \frac{d\beta}{d\omega}\bigg|_{\omega=\omega_0} = \frac{1}{v_g}, \tag{2.2}$$

where v_g is the group velocity and

$$\beta_2 = \frac{d^2\beta}{d\omega^2}\bigg|_{\omega=\omega_0} = -\frac{1}{v_g^2}\frac{dv_g}{d\omega}. \tag{2.3}$$

β_2 is also known as the GVD parameter. Eqn. (2.1) can be simplified to

$$i\frac{\partial A}{\partial z} = -\frac{i}{2}\alpha A + \frac{1}{2}\beta_2\frac{\partial^2 A}{\partial T^2} - \gamma|A|^2 A, \tag{2.4}$$

where

$$T = t - \frac{z}{v_g}. \tag{2.5}$$

To normalize the time scale, τ is introduced, where

$$\tau = \frac{T}{T_0} \tag{2.6}$$

and T_0 is the rms width of the envelope (pulse) at z=0.

To normalize the amplitude of the pulse we define

$$A(z,\tau) = \sqrt{P_0}\exp(-\alpha z/2)U(z,\tau), \tag{2.7}$$

where P_0 is the peak power of the incident pulse and $U(z,\tau)$ is the normalized amplitude. Thus from eqn. (2.4) the normalized amplitude satisfies the equation

$$i\frac{\partial U}{\partial z} = \frac{sgn(\beta_2)}{2L_d}\frac{\partial^2 U}{\partial \tau^2} - \frac{\exp(-\alpha z)}{L_{nl}}|U|^2 U, \tag{2.8}$$

where $sgn(\beta_2)$ is $+1$ or -1 depending on the sign of β_2 and L_d is given by

$$L_d = \frac{T_0^2}{|\beta_2|}, \tag{2.9}$$

and

$$L_{nl} = \frac{1}{\gamma P_0}. \tag{2.10}$$

These definitions lay a foundation for the rest of the analytical explanation.

2.2 Group velocity dispersion and Self phase modulation

Group velocity dispersion (GVD) occurs due to the fact that in a particular medium, different spectral components travel at different speeds. A pulse will maintain its width only if all the spectral components arrive at a point at the same time. In fiber, this is not the case and GVD occurs causing pulse broadening. The coefficient of dispersion D can be related to the GVD parameter β_2 by

$$D = -\frac{2\pi c}{\lambda^2}\beta_2.$$

(2.11)

Depending on the sign of β_2, two dispersion regimes can be identified - normal and anomalous. The 'normal' dispersion regime is when $D<0$, $\beta_2>0$ i.e. GVD is positive and $\lambda<\lambda_0$ where λ_0 is the zero dispersion wavelength. It is seen that in this case, higher frequency components of an optical pulse are slower than the lower frequency components. The opposite occurs for negative GVD or in the so-called anomalous regime. Here $D>0$, $\beta_2<0$ and $\lambda>\lambda_0$.

To see the effect of GVD and SPM, eqn. (2.8) must be solved. In general eqn. (2.8) cannot be solved, therefore we consider two cases 1) Dispersion alone (i.e. L_{nl} is infinite) and 2) Nonlinearity alone (i.e. L_d is infinity).

2.2.1 Dispersion alone

Setting L_{nl} equal to infinity in eqn. (2.8) and using eqn. (2.9), we find that for a linear dispersive medium, $U(z,T)$ satisfies

$$i\frac{\partial U}{\partial z} = \frac{1}{2}\beta_2 \frac{\partial^2 U}{\partial T^2}.$$ (2.12)

It can be shown [4] that GVD shifts the phase of each component of the pulse and although this phase change does not alter the spectrum of the pulse it may modify the pulse shape. For example, although a Gaussian pulse maintains its shape when propagating, its width increases. This increase is given by

$$T = T_0[1 + (\frac{z}{L_d})^2]^{1/2}.$$ (2.13)

Thus when $z=L_d$, the Gaussian pulse broadens by a factor of $\sqrt{2}$.

2.2.2 Nonlinearity alone

When only the nonlinearity is present, setting $\beta_2 = 0$, in eqn. (2.8) gives

$$\frac{\partial U}{\partial z} = \frac{i}{L_{nl}}\exp(-\alpha z)|U|^2 U.$$ (2.14)

The solution of eqn. (2.14) is given by

$$U(z,\tau) = U(0,T)\exp(i\phi_{nl}(z,T)),$$
(2.15)

where ϕ_{nl} is the nonlinear phase shift and $U(0,T)$ is the field amplitude at z=0. ϕ_{nl} is a function of distance and time and is given by

$$\phi_{nl}(z,T) = |U(0,T)|^2 (z_{eff} / L_{nl}).$$
(2.16)

z_{eff} is the effective length of the fiber (which is of length z), taking attenuation into consideration,

$$z_{eff} = \frac{1}{\alpha}(1-\exp(-\alpha z)).$$
(2.17)

If discrete equally spaced optical amplifiers are used, then the effective distance between amplifiers is given by (2.17) with $z = z_{amp}$. z_{amp} is the distance between amplifiers. In a long system of length z, there are $\dfrac{z}{z_{amp}}$ amplifiers, so the total effective length is then given by

$$z_{eff} = \frac{(1-\exp(-\alpha z_{amp}))}{\alpha} \frac{z}{z_{amp}}.$$
(2.18)

In a system with optical amplifiers, (2.18) gives the expression for z_{eff} that is used in (2.16). Note that z_{eff} is less than z because the optical power decreases between amplifiers and the effective average power, $\overline{P}$, is less than the peak power P_0.

$$\overline{P}z = P_0 z_{\text{eff}}. \tag{2.19}$$

From eqn. (2.16) we see that the phase shift due to SPM depends on L_{nl} which in turn depends on the incident power. Actually, it is proportional to the incident power. The phase shift increases with distance as well. The maximum phase shift is given by

$$\phi_{\max} = \frac{z_{\text{eff}}}{L_{\text{nl}}} = \gamma P_o z_{\text{eff}}. \tag{2.20}$$

Thus L_{nl} is the effective propagation distance at which the maximum phase shift is 1 rad.

Since the SPM induced phase is a function of time, it is obvious that the optical frequency will also vary about a certain frequency ω_0 and be a function of time. This time dependent variation in frequency is known as a frequency chirp. The frequency chirp is given by

$$\delta\omega(T) = -\frac{\partial\phi_{nl}}{\partial T} = -\frac{\partial|U(0,T)|^2}{\partial T}\frac{z_{\text{eff}}}{L_{nl}}. \tag{2.21}$$

Thus we note that the induced frequency chirp is proportional to the derivative of the square of the magnitude of the initial pulse. Eqn. (2.21) will play an important role when designing the parameters for the circuit model.

The frequency chirp due to SPM is such that the leading edge of the pulse has lower frequencies and the trailing edge has higher frequencies (Fig. 1). The first diagram in Fig. 1 shows the time variation of the signal when affected by SPM while the second diagram shows the frequency variation. SPM causes the input signal to break up in both the time and frequency domains. Fig. 2 gives the frequency spectra of a Gaussian signal for different values of maximum phase shift.

2.2.3 Combined effect of GVD and SPM

Now we consider the combined effect of GVD and SPM. Eqn. (2.8) can be written as

$$i\frac{\partial U}{\partial \xi} = sgn(\beta_2)\frac{1}{2}\frac{\partial^2 U}{\partial \tau^2} - N^2 e^{-\alpha z}|U|^2 U,$$ (2.22)

where $\xi = z/L_d$ and $N^2 = L_d/L_{nl}$.

Typically for most fiber optic systems, dispersion is much more significant than nonlinear effects ($L_d \ll L_{nl}$), consequently, $N \ll 1$. For example, in a typical terrestrial fiber optic system operating in the 1.3 µm window, D is approximately 1 ps/km.nm. At a bit rate of
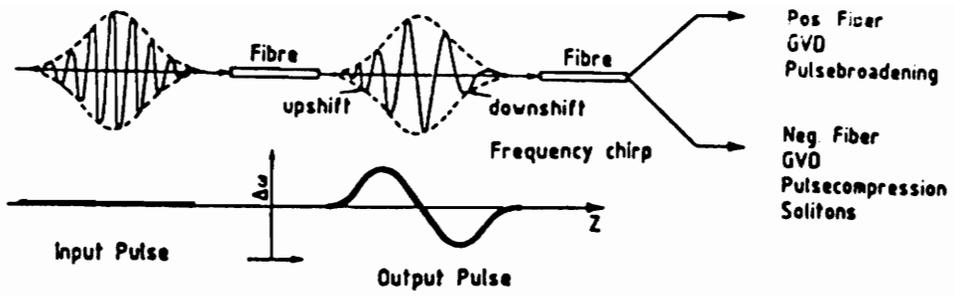
Figure 1. SPM in fiber - time variation and frequency variation[5]
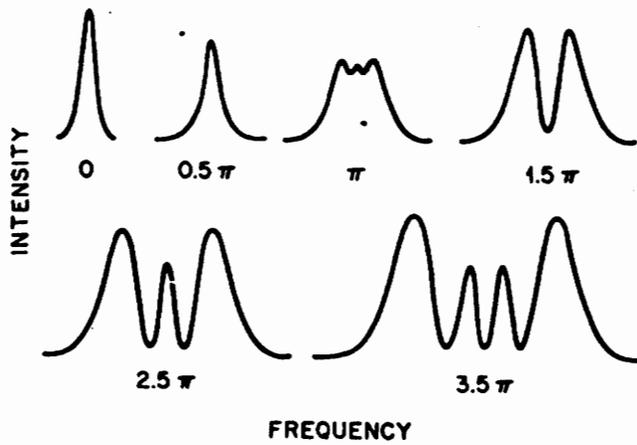

Figure 2. SPM-broadened spectra for an unchirped Gaussian pulse for different phase

shifts[4]

2.4 Gb/s, this would correspond to L_d = 9034.4 km. For an input power of 1 mW, L_{nl} is found to be 386.1 km considering the nonlinearity constant to be 2.59x10^{-3} /Wm. For undersea links, long distances must be traversed and so dispersion is kept low. Thus L_d is very large, N>>1 and SPM dominates. As described previously, positive GVD coupled with SPM increases the width of the pulse. For a Gaussian input pulse, the broadening ratio is given by [4]

$$\frac{\sigma}{\sigma_0} = [1 + \sqrt{2}\phi_{max}\frac{z}{L_d} + (1 + \frac{4}{3\sqrt{3}}\phi_{max}^2)\frac{z^2}{L_d^2}]^{1/2}. \tag{2.23}$$

This relation is plotted in Fig. 3 for z/Ld ranging from 0 to 3, nonlinear constant = 2.59x10^{-3} /Wm and incident power equal to 0.5 and 5 mW. It is seen that an increase in power increases the broadening ratio since nonlinear length is decreased. As z/Ld increases the broadening ratio increases to a greater extent.

When this effect is coupled with positive GVD, the lower frequencies tend to speed up causing the front of the pulse to pull away while the higher frequencies tend to slow down causing the trailing edge of the pulse to fall back further. Thus pulse broadening increases. When SPM is coupled with negative GVD, compensation occurs and solitons [1,10] may be formed.
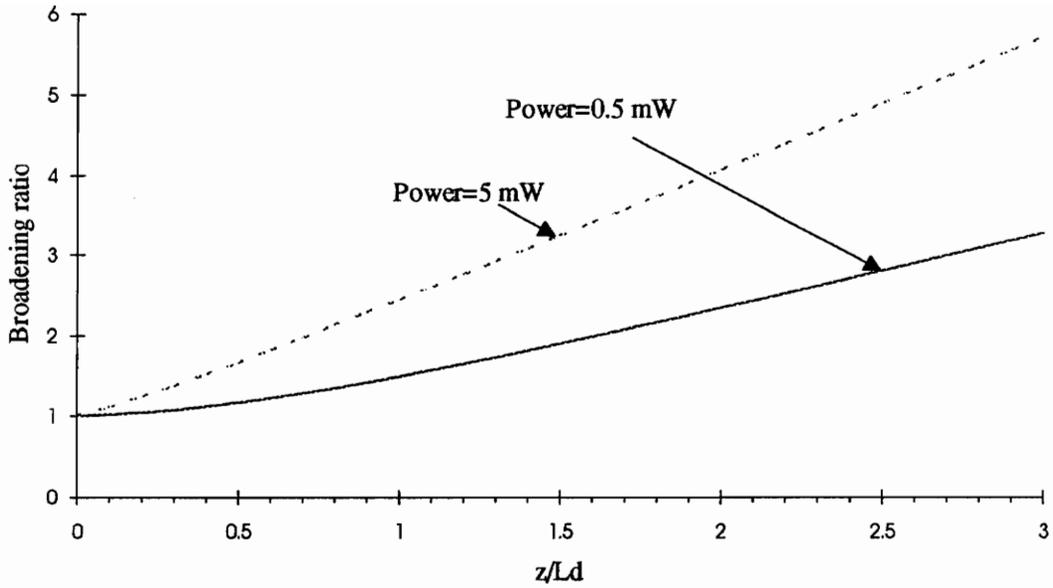
Figure 3. Broadening ratio vs. z/Ld for a Gaussian pulse

2.3 The lightwave system

A model is designed that can support the simulation of different lightwave systems having different parameters. It is useful to consider a baseline case as given in Table 1.

Table 1. Lightwave System Parameters

Parameter	Value
Bit-rate	10 Gb/s
Attenuation	0.25 dB/km

Wavelength	1550 nm
Coefficient of Dispersion	-0.04 ps/km.nm
Nonlinearity Constant	2.59×10^{-3} /W.m
Input power	1 mW

When simulating the system, the main assumptions made are:

• Dispersion due to polarization is not considered.

• Higher orders of dispersion, i.e. terms beyond β_2, are considered to be negligible.

• No noise is considered in the system.

• The attenuation of the fiber has been implicitly considered in the use of z_{eff}. The effect of this approximation could be simulated but it is not expected to be of importance. This is because, to avoid taking amplifier noise into consideration, the gain of the amplifiers that are considered to be used in the system is low (about 10 dB) and so the approximation is good. Attenuation can be modeled explicitly by incorporating an attenuator.

• A transform-limited input pulse is considered, i.e. the spectral width of the input is determined by the pulse modulation and not by the spectral width of the carrier.

The fiber link can be viewed as shown in Fig. 4. Here a continuous system is modeled as a set of discrete identical systems in tandem.
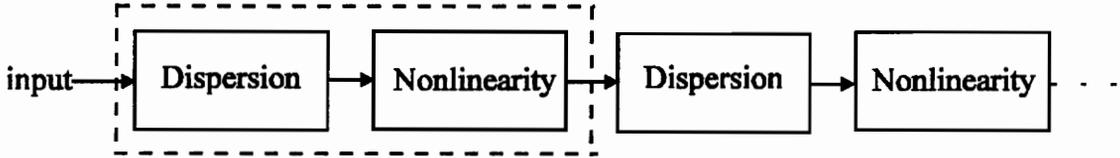

Figure 4. Fiber Model

Consider the transfer function of the portion enclosed in dotted lines to be H(w). Then the transfer function after n such blocks is H^n(w). For a single isolated pulse, this transfer function can be obtained by a single block with transfer function H(w) and a feedback loop having a delay T. The transfer function (TF) then becomes

$$TF = \frac{H(w)}{1 - e^{-jwT} H(w)} = H(w)[1 + e^{-jwT} H(w) + e^{-2jwT} H^2(w) + \ldots].$$

(2.22)

Thus each term can be isolated provided T is greater than the width of h(t), where h(t) is the impulse response of the single block. This enables the pulse response of a long system to be simulated by looping around a short system. This 'loop back' technique has been widely used [6] to estimate the behavior of very long fiber optic systems.

Chapter 3: Circuit Design

3.1 Components of the circuit

Fig. 5 shows the block diagram of the circuit designed to model the effect of dispersion and nonlinearity in fiber. The components and frequency range were chosen such that implementation of the circuit would be possible. The basic explanation of the circuit is as follows.   An initial pulse is fed into the system, which is then modulated by a high frequency carrier.   This modulated signal is passed through a dispersive bandpass Butterworth filter that spreads the signal out in time. The effective action of this filter is to model dispersion. Since the frequency chirp due to SPM depends on the intensity of the signal, an envelope detector is introduced to extract the envelope. This signal is then normalized and squared according to eqn. (2.21). Since a change in phase is required, a differentiator is placed before the VCO. An FM modulator preceded by a differentiator gives a phase modulator. The output of the VCO is then multiplied by the output of the bandpass filter to recover a baseband signal, retaining the phase change. This signal is then delayed and fed back into the system. It is modulated by the carrier once again and sent through the system.
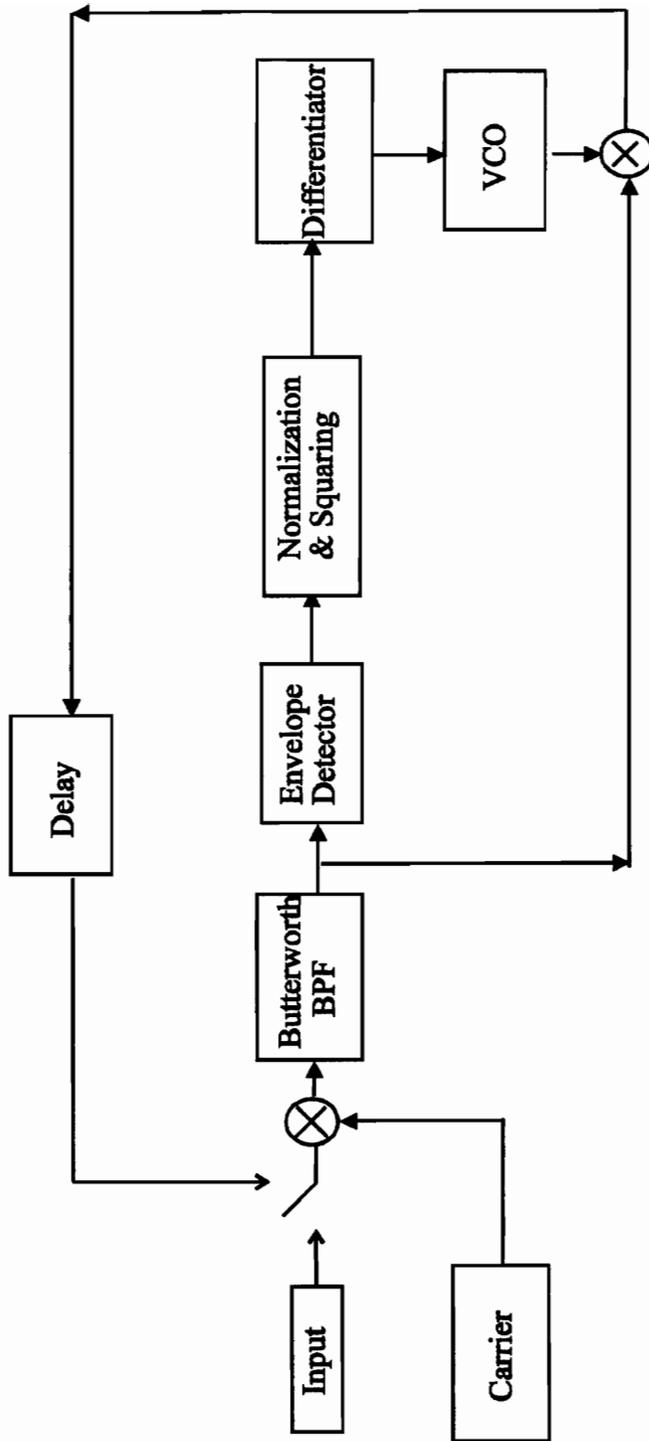
Figure 5.   System Block Diagram

The original input pulse is isolated from the system by a switch. A detailed explanation of the working of the circuit is given in section 3.2.

The main components of the system are:

• Butterworth bandpass filter:

The Butterworth bandpass filter models dispersion in the fiber. A Butterworth filter was chosen as it has a maximally flat magnitude response in the passband. It has a bandwidth of 40 MHz and a center frequency of 70 MHz. The filter order was designed to be 4. Fig. 6a-6d shows some of the characteristics of the filter designed.
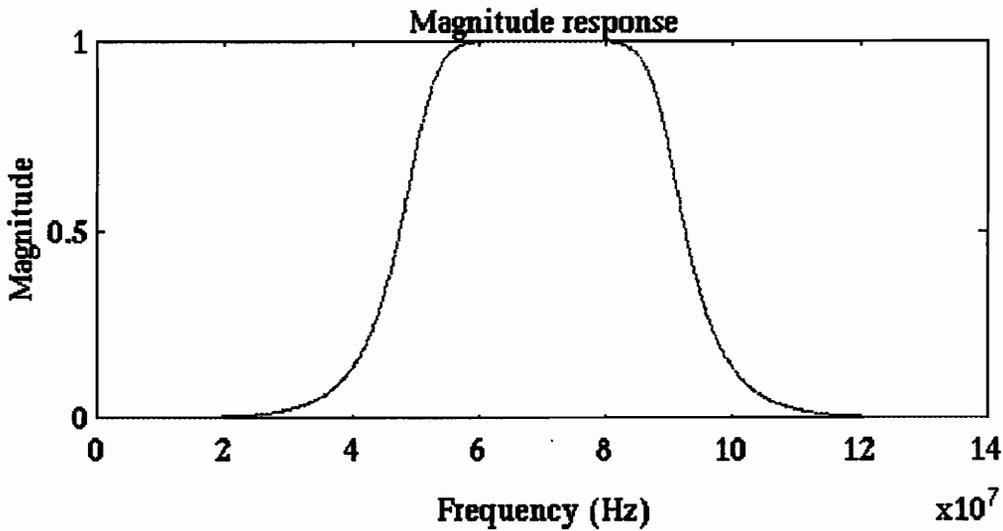

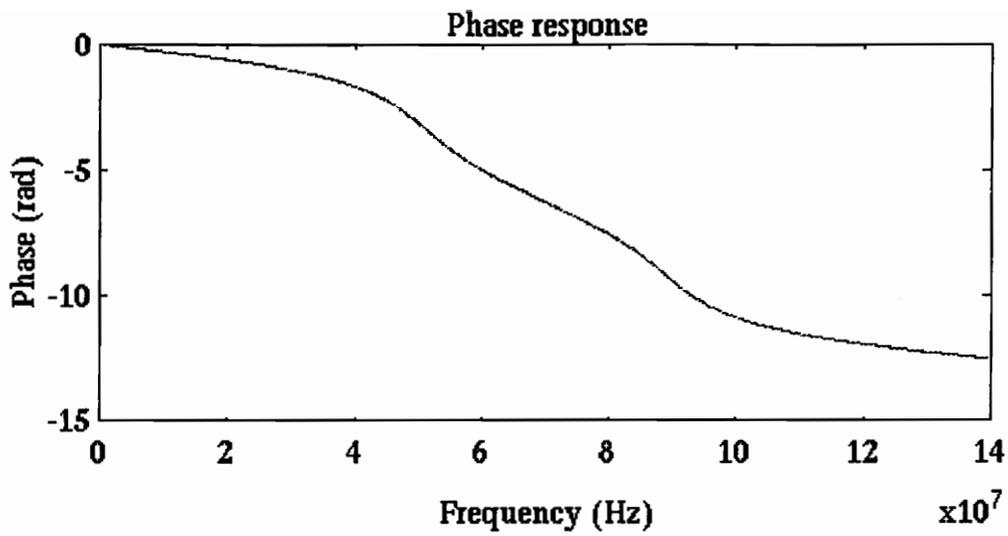Figure 6a. Magnitude response of the bandpass Butterworth filter

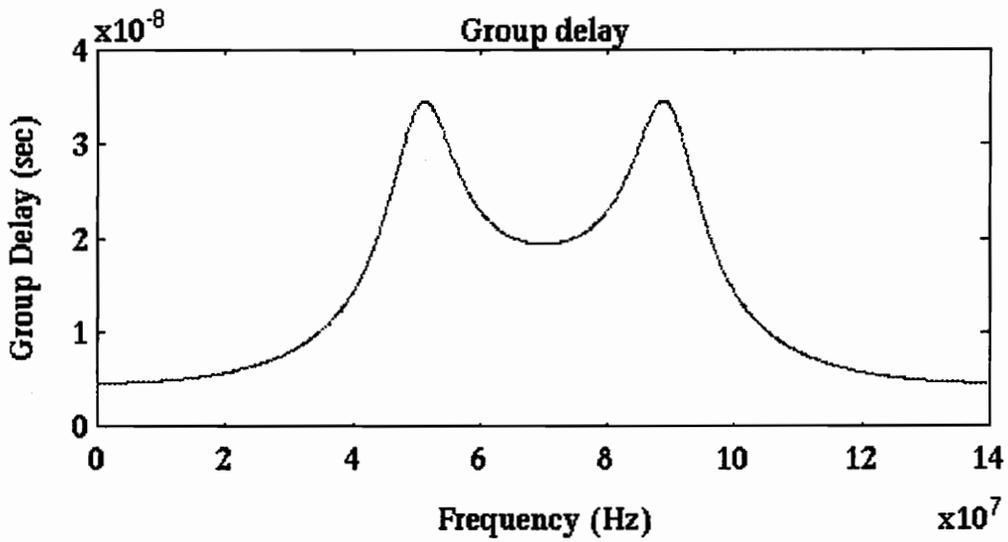Figure 6b. Phase response of the bandpass Butterworth filter

Figure 6c. Group delay for the bandpass Butterworth filter

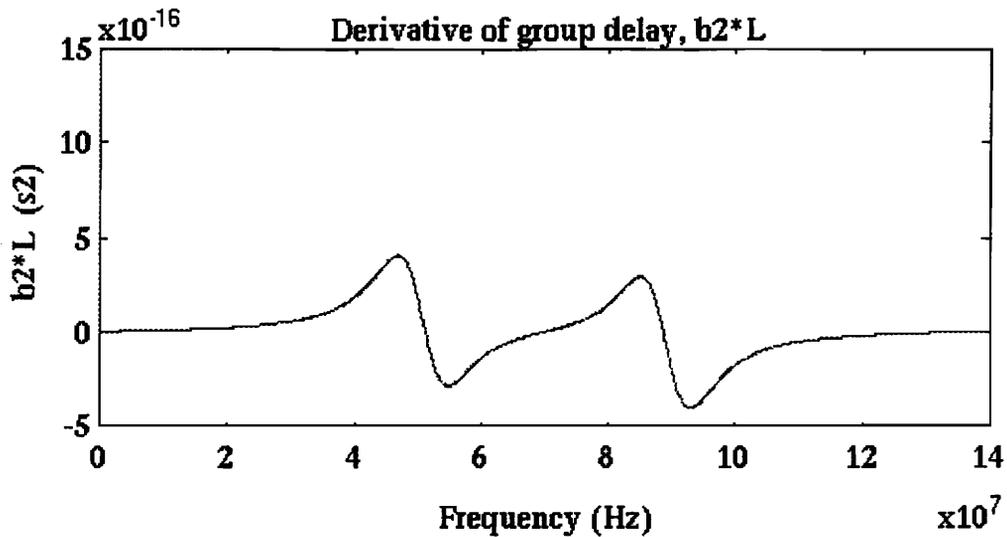Figure 6d. $\beta_2 L$ vs. Frequency for the bandpass Butterworth filter

• Envelope Detector:

The envelope detector consists of a module that gives the absolute value of the input and is followed by a Butterworth low-pass filter. The filter has a 3 dB bandwidth of 40 MHz and is of order 6. This filter removes the high frequency carrier, thus giving the envelope of the signal.
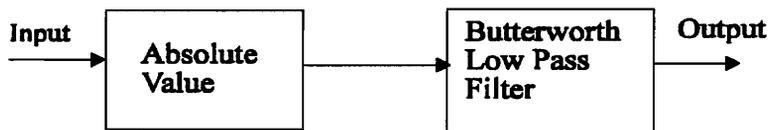

Figure 7. Envelope detector

• Differentiator:

The differentiator consists of basic arithmetic blocks that implement the definition of a derivative. Each sample of the input is subtracted from the next sample and this difference is divided by the sample time.

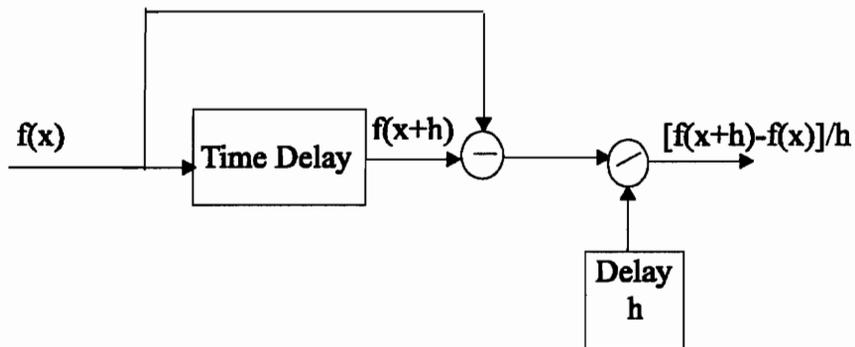Figure 8. Differentiator

• Voltage controlled oscillator (VCO):

The VCO is used to simulate the frequency chirp induced by the SPM. The free-running frequency is such that the dispersion introduced by the filter at this frequency is equal to the desired dispersion in the fiber. This will be explained in detail in (3.2). The VCO free running frequency is 83.41 MHz.

3.2 Working of the circuit

The input is a time-limited signal. It is a half sinusoid having a period of 0.5 μs. In BOSS it is obtained by gating a sinusoidal signal of frequency 1 MHz by a unit square pulse of 0.5 μs duration. The baseband signal is then upshifted in frequency using a sinusoid carrier of frequency 83.41 MHz. The signal is then passed through a bandpass filter to spread the signal out. To ensure that the dispersion is as desired, consider the following calculations.

$\beta_2 L$ for the fiber can be calculated from the parameters given in Table 1. By normalizing all quantities to dimensionless parameters, it is possible to obtain a direct correspondence between the simulation and the fiber system. The appropriate normalized quantity for $\beta_2 L$ is $\dfrac{\beta_2 L}{(\text{Bit period})^2}$. For the fiber system

$$\frac{\beta_2 L}{(\text{Bit Period})^2} = 1.01965 \times 10^{-3}.$$

It is required that

$$\left[\frac{\beta_2 L}{(\text{Bit period})^2}\right]_{\text{fiber}} = \left[\frac{\beta_2 L}{(\text{Bit period})^2}\right]_{\text{simulation}}, \qquad (3.1)$$

where bit period of the fiber system is 0.1 ns and that of the simulation is 0.5 μs.

Thus, $(\beta_2 L)_{simulation} = 2.5491 \times 10^{-16} \, s^2$.

From the characteristics of the filter shown in Fig. 6d, the frequency at which $\beta_2 L$ is the required value is 83.41 MHz. This value sets the carrier frequency and the free-running frequency of the VCO. The output of the filter is then sent through an envelope detector which recovers the envelope of the pulse. The dispersed pulse then is affected by the nonlinearity. To obtain SPM induced frequency chirp (refer to eqn. (2.21)), the signal is first normalized and squared. It is then differentiated and negated. This signal controls the frequency of the output of the oscillator. It then follows from eqn (2.21) that the VCO constant, i.e. the conversion constant between the voltage of the input and the frequency of the output is set to be the ratio of z_{eff} to the nonlinear length. Given the attenuation of the fiber, the loss per pass is 50 dB. If amplifiers of gain 10 dB are used, the distance between amplifiers is calculated to be 40 km. Using eqn (2.19) and the relation

$$\alpha \, dB/km = 4.34 \, \alpha \, /km, \tag{3.2}$$

z_{eff} for $z = 200$ km is found to be 118.75 km. From the baseline case ($P_0 = 1mW$), $L_{nl} = 386.1$ km and the VCO constant is equal to 0.3076. The output of the VCO is then multiplied by the original product modulated signal. The baseband signal obtained is then fed back into the system. The original pulse has now been affected by both dispersion and nonlinearity. When the signal passes through the system again the signal further broadens due to dispersion and the frequency chirp and phase shift induced in the present pass of the system is coupled with the effect of SPM in the previous pass. A time delay is introduced

in the feedback path so that the pulses do not merge together and observation of the pulse is facilitated.

The circuit has been designed such that various parameters can be changed, giving it flexibility. The dispersion-limited distance can be changed by varying the carrier and free running frequency of the VCO. The nonlinear-limited distance can be changed by varying the VCO constant. By decreasing the delay in the feedback loop, the effect of inter-symbol interference between consecutive pulses could be studied. The bit rate of the simulation can be varied by changing the frequency of the input sinusoid and the time period of the gating pulse. Thus, the circuit designed seems to model the required system well.

3.3 Obstacles and precautions

When designing the system for simulation, some difficulties arose not only due to the components chosen but also due to the constraints of the simulation. Some of the main obstacles are stated below.

• The sampling frequency of the simulation is very critical and should be chosen such that the sinusoidal carrier retains its shape. Undersampling would distort the signal and would change the subsequent pulse shape. To overcome this, the sampling frequency could also be made an integral multiple of the sinusoidal frequency or a frequency very much larger than twice the highest frequency of operation is chosen. The former was

chosen, since we are limited by memory restictions in the simulation of very long systems

- The bandwidth of the envelope detector should be selected such that the high frequency carrier is eliminated.

- There are some disadvantages of using a filter in the design. Consider a filter having a transfer function of the form $A(\omega)e^{j\theta(\omega)}$. Due to the loop configuration of the circuit, after n loops the transfer function becomes $A^n(\omega)e^{jn\theta(\omega)}$. Although a maximally flat filter response is used, there are some unavoidable variations in $A(\omega)$ when there is phase dispersion. This small variation is magnified when $A(\omega)$ is raised to a high power. An ideal fiber is generally modeled by a phase variation and no amplitude variation, but this is non-causal. Also, the optical amplifiers introduce some amplitude variation. Thus, it is felt that the amplitude variation in the simulation may correspond more closely to the physical situation than idealized theoretical models.

Chapter 4: Simulation and Results

4.1 BOSS Simulation

BOSS is a software tool that is used for simulation based analysis and design of systems. It oversees all software functions that are necessary to build simulation models, execute simulations, view simulation results and perform design iterations [7]. BOSS consists of basic functional blocks that can be integrated to form a system that performs the task desired. A FORTRAN simulation code is generated from the block diagram representation and the simulation is executed without user intervention. Thus the user designs subsystems and functional modules, without the need for an intermediate language for describing the topology of the system. The user must specify the value of the required parameters so that the system can be defined explicitly. The value of these parameters can be easily changed so as to incorporate flexibility in the simulation. The points in the system at which the signal is to be observed can be specified. The simulation results are then stored and can be viewed in a large number of ways (magnitude response, phase response, time plot, scatter plot etc.). BOSS was found to be a user-friendly and intelligent software package [7].

Using BOSS, the circuit model explained in chapter 3 was simulated. Long distance links should be designed for small values of dispersion. We first look at the effect of a low coefficient of dispersion and no nonlinearity. Fig. 9 shows the BOSS block diagram for this case. We then look at the effect when nonlinearity is added. Since the effect of nonlinearity is to be studied, L_d is designed to be larger than L_{nl}. L_{nl} is then varied by changing the input power. Fig. 10 shows the BOSS block diagram for the case of dispersion and nonlinearity combined. The cases that are studied are:

Case (1) D=-0.04 ps/km.nm, no nonlinearity

Case (2) D=-0.04 ps/km.nm, nonlinearity considered, incident power=3 mW

Case (3) D=-0.04 ps/km.nm, nonlinearity considered, incident power=5 mW

Case (4) D=-0.04 ps/km.nm, nonlinearity considered, incident power=7 mW

Although the thrust has been on systems having low positive GVD and significant nonlinearity, it is interesting to study the effect of increasing the amount of dispersion and comparing it to results obtained for a lower dispersion but the same nonlinearity. This was done for the following case.

Case (5) D=-0.4 ps/km.nm, nonlinearity considered, incident power=5 mW
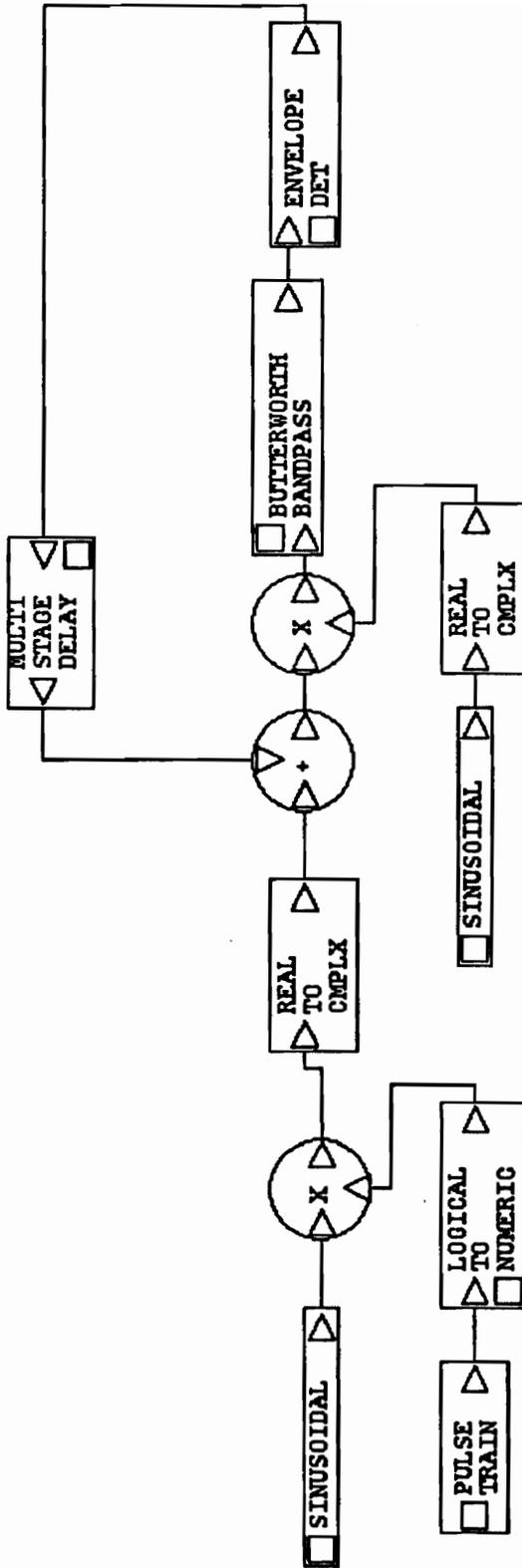
4.2 Results

We now look at each case individually.
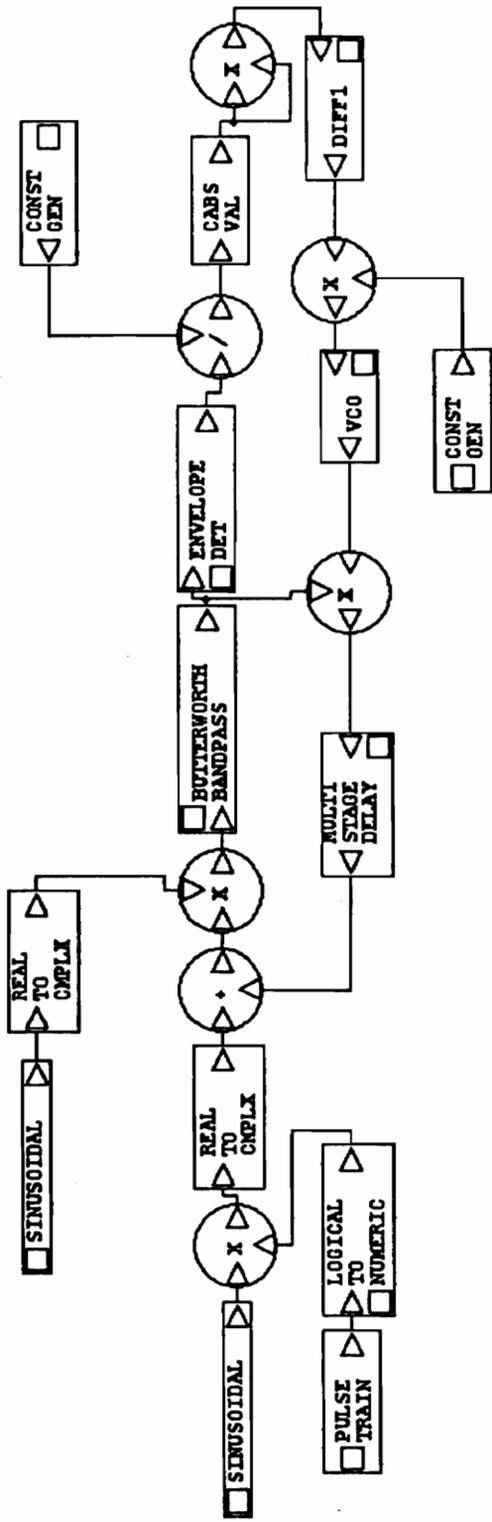
Figure 9. BOSS block diagram for dispersion alone

Figure 10. BOSS block diagram for dispersion and nonlinearity

Case (1) D=-0.04 ps/km.nm, no nonlinearity

First the case of dispersion alone was studied. L_d was found to be 9155 km. Referring to Fig. 9, the 10 dB bandwidth of the pulse at the output of the envelope detector was measured and the ratio of this value to the 10 dB bandwidth of the original pulse was calculated. This is taken to be the broadening ratio. Each loop of the circuit corresponds to 200 km and depending on how many passes of the circuit are considered, the distance can be determined. Fig. 11 shows the output of the envelope detector for the first 7 passes. Although the broadening is not obvious from the plot, on magnifying each pulse and measuring the 10 dB bandwidth, the broadening ratio is obtained. Fig. 12 shows the real output of the bandpass Butterworth filter. The theoretical value of the broadening ratio for a Gaussian pulse was calculated using eqn. (2.13).

A graph of broadening ratio versus distance was plotted and is shown in Fig. 13. Since the theoretical calculation is for a Gaussian input pulse shape and for the rms pulse width, the simulated and theoretical values are expected to differ in value. From eqn (2.13), for a Gaussian pulse, the broadening ratio increases more rapidly with increasing distance. Although as distance increases the broadening ratio of the sinusoidal pulse increases, it tends to increase at a slower rate then that of the theoretical calculations for the Gaussian pulse. This could be due to a number of reasons. The most plausible reason may be associated with the considerably different spectral characteristic of the sinusoidal and Gaussian pulses. It could also be due to amplitude variations in the filter characteristics as discussed in section 3.3. This could narrow the effective spectrum of the pulse, and thereby decrease the rate at which the dispersion increases.
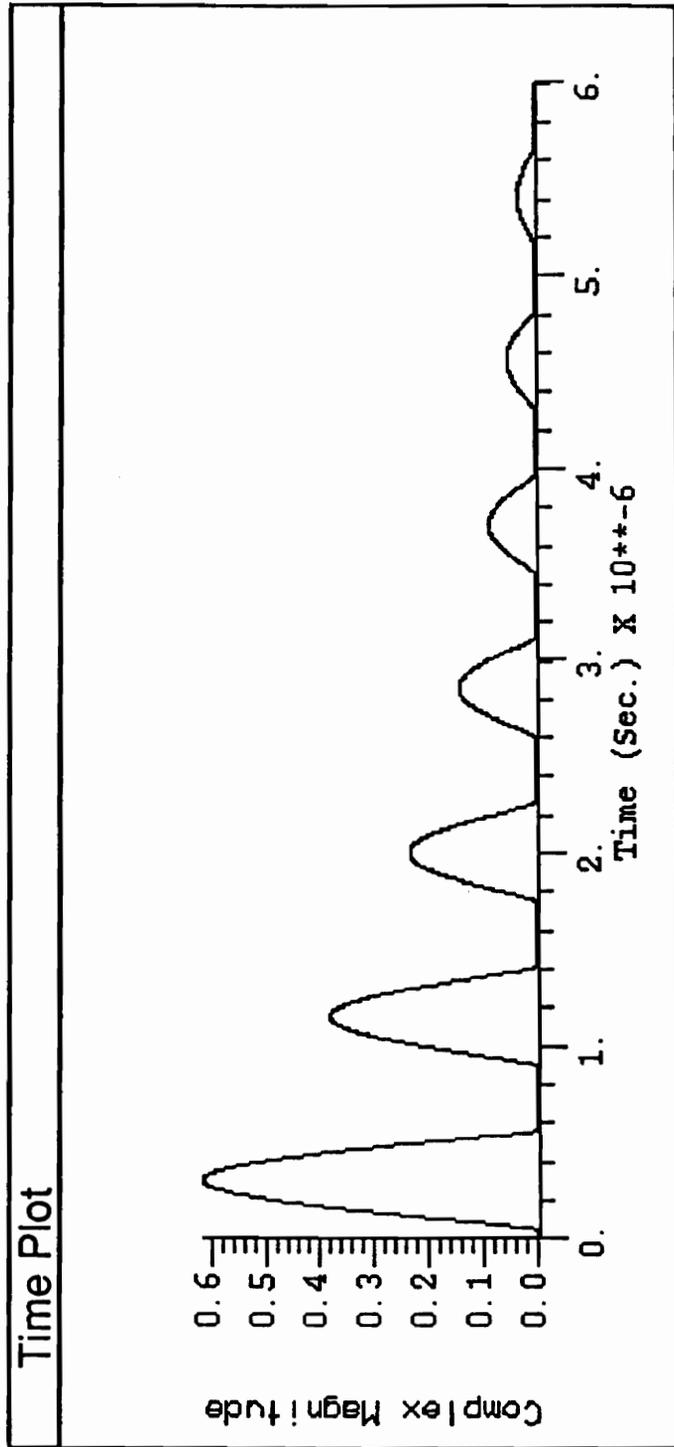
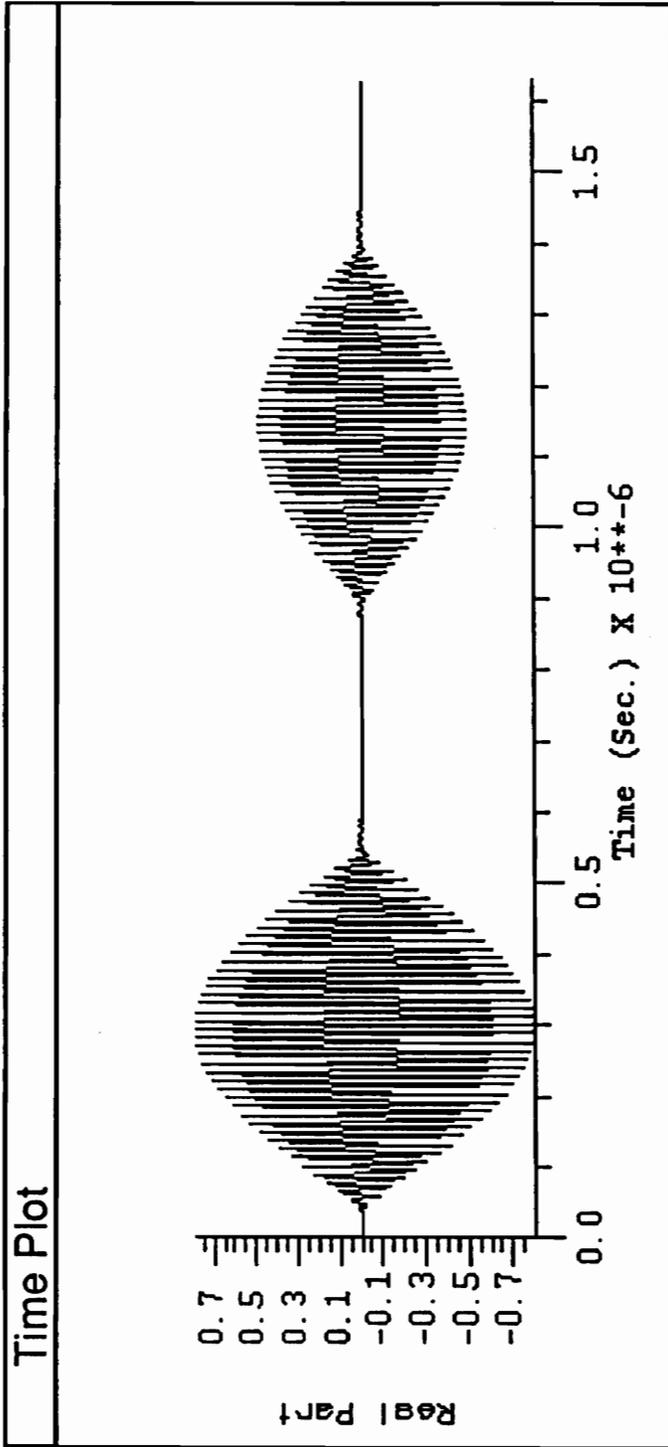Figure 11. Dispersed output for the first 7 passes of the circuit

Figure 12. Real output of the bandpass Butterworth filter for the first two passes
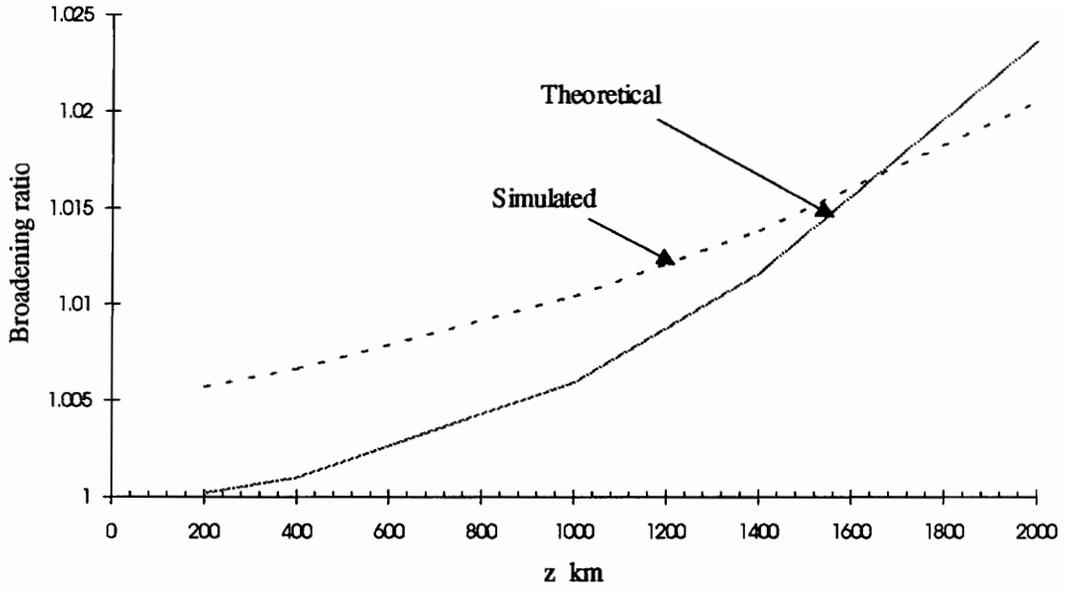
Figure 13. Broadening ratio vs. Distance for case (1) - dispersion alone

The filters (both that in the envelope detector and the Butterworth bandpass filter) were replaced by a model in which the phase and magnitude could be specified for a range of frequencies, i.e. a frequency domain filter, but the same results were obtained. Some anomaly may be occuring due to the loop configuration. It is important to note that after 10 loops the effect of nonlinearity overpowers that of dispersion and thus for the purpose of this simulation, the model for dispersion is adequate.

Now the combined effect of dispersion and nonlinearity is investigated. The BOSS block diagram for this is provided in Fig. 10. Fig. 14 shows the input to the system. Fig. 15 shows an example of the output phase variation of the VCO for an input power of 3 mW.

Case (2) D=-0.04 ps/km.nm, nonlinearity considered, incident power=3 mW

Fig. 16 shows the output of the fourth to eighth pass. In this case, the nonlinear length L_{nl} is calculated from eqn. (2.10). It was found to be 128.7 km. From eqn. (2.9), L_d is 9155 km. Thus the value of N in eqn. (2.22) is 8.434. The effect of nonlinearity is not very severe for at least 8 passes. As seen in Fig. 17, for 18 passes (3600 km) there begins to be a splitting of the pulse. Due to SPM, high frequency components are induced. This causes the main lobe to become narrower but the overall width of the pulse increases. The pulse width was calculated and compared to the broadening ratio of a Gaussian pulse given in eqn. (2.23). Fig. 18 shows a plot of the broadening ratio vs. the distance. A difference is expected between the theoretical and simulated values as the pulse shapes are
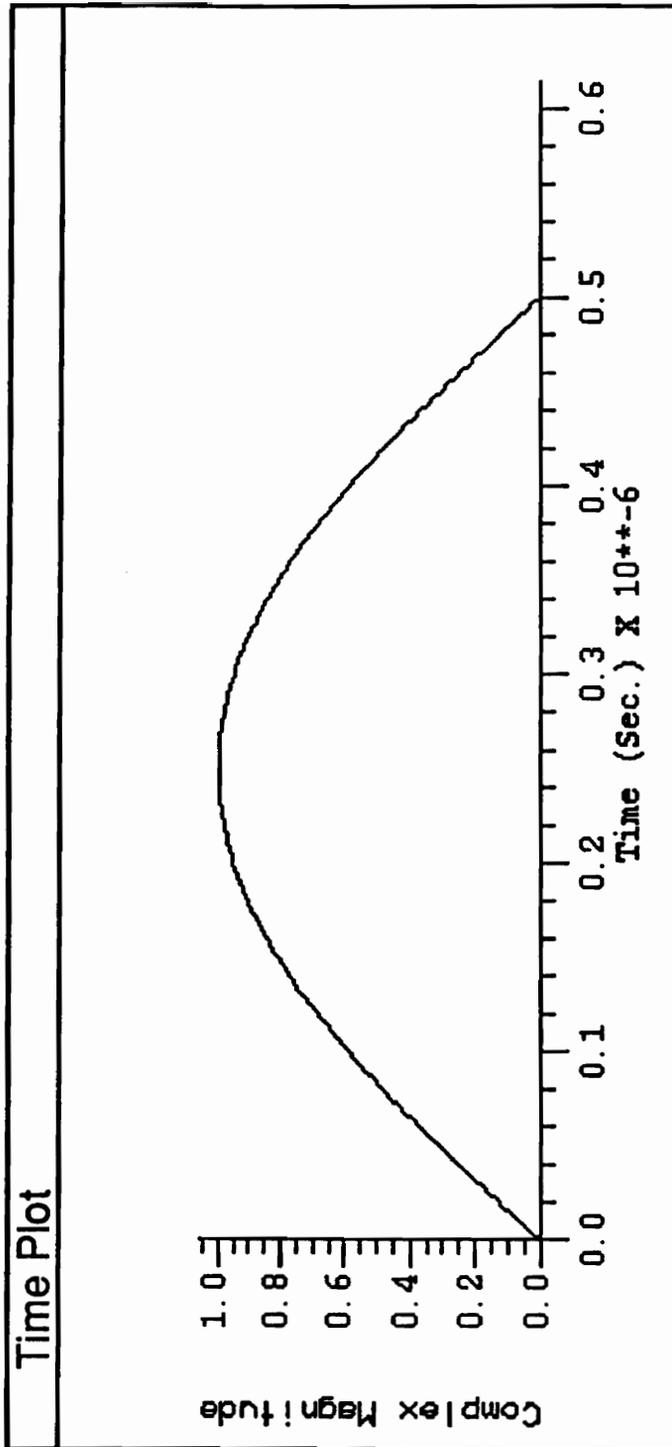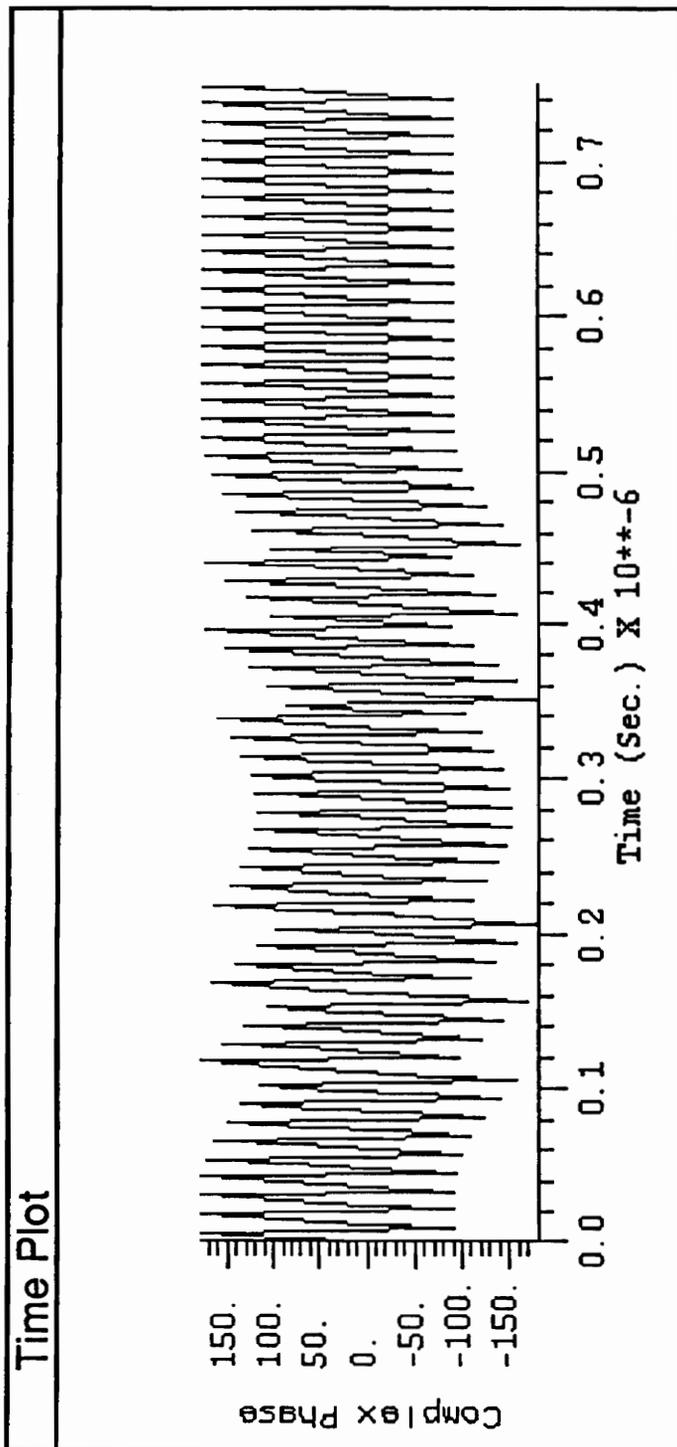
Figure 14. Input pulse to the system

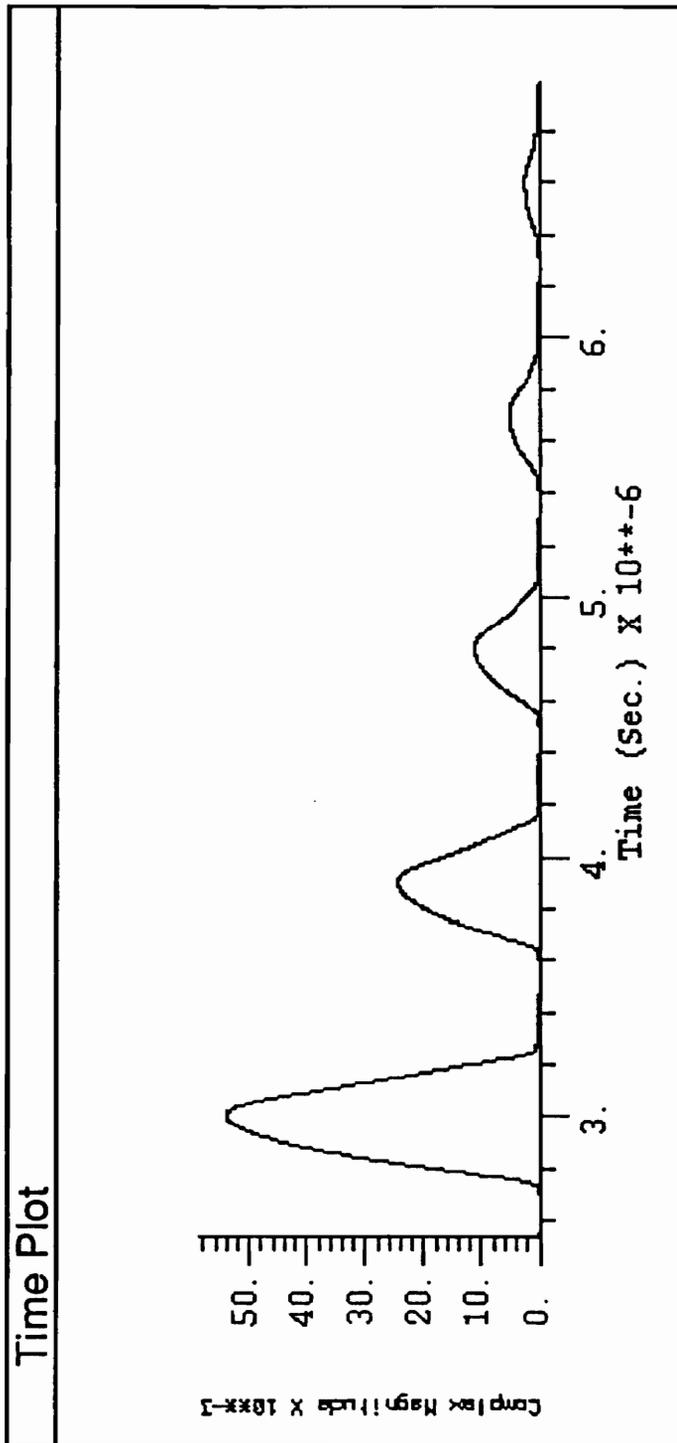Figure 15 Output phase of the VCO for the first pass

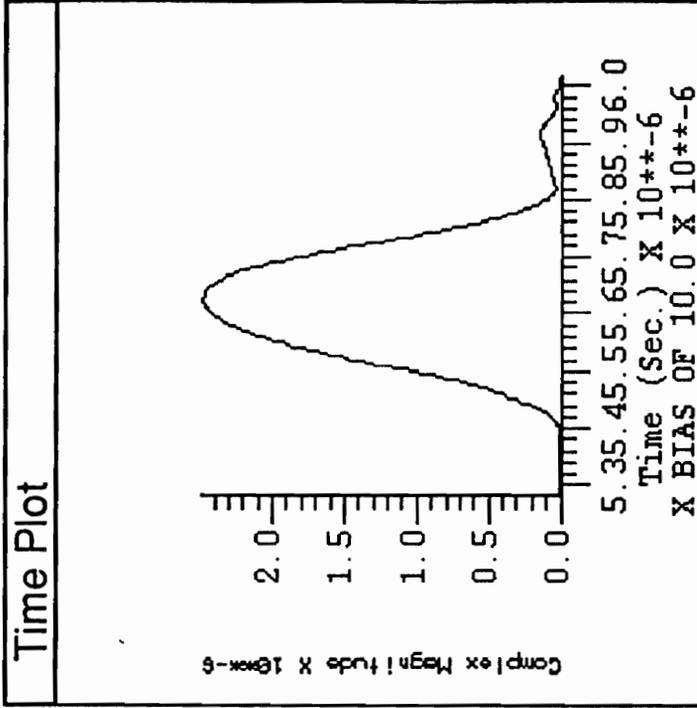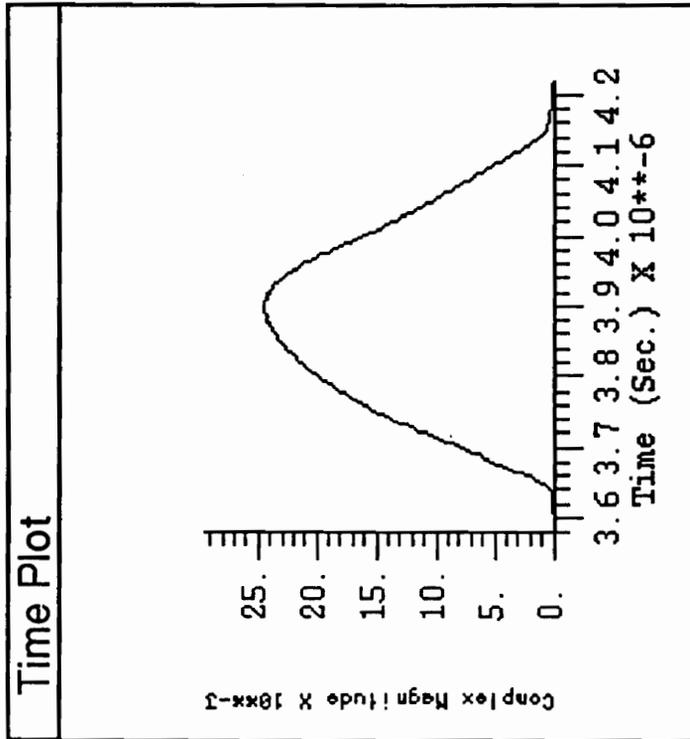Figure 16 Ouput for case (2) - dispersion and nonlinearity, pass 4 to 8, pwr=3 mW

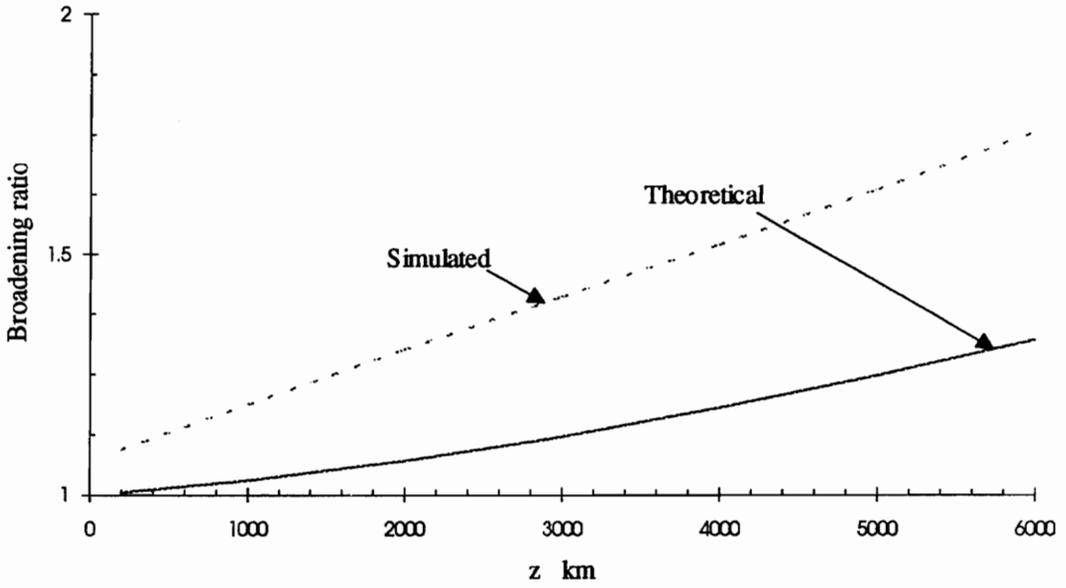Figure 17. Output for case (2), for pass 5 and 18

Figure 18. Broadening ratio vs. Distance for case (2)

different. As discussed, frequency chirp occurs mainly in the leading and trailing edges. As seen in [4], as edges become steeper the pulse spreads out more, in the time domain. Thus since a sinusoid of certain width has steeper sides than a Gaussian of the same width, the broadening may be larger.

Case (3) D=-0.04 ps/km.nm, nonlinearity considered, incident power=5 mW

Fig. 19 shows the output of the first seven passes. In this case L_{nl} is 77.22 km and N is 10.89. The effect of nonlinearity is more pronounced as compared to the case for an input power of 3 mW. This is due to the decrease in nonlinear length and thus an increase in SPM distortion. In Fig. 20, we see that for even the fifteenth pass of the circuit (3000 km) the distortion is more than that of the eighteenth pass in case (2). Fig. 21 shows a plot of the broadening ratio vs. distance for the theoretical Gaussian case and the simulation. The two curves agree closely but as discussed in case (2) an offset is seen.

Case (4) D=-0.04 ps/km.nm, nonlinearity considered, incident power=7 mW

Fig. 22 shows the pulse obtained for the first to seventh pass. Compared to case (2) and case (3), it shows the most distortion. In this case L_{nl} is 55.16 km and N is 12.88. Thus it is found that by increasing the input power i.e. decreasing the nonlinear length and increasing N, distortion due to SPM increases. Fig. 23 shows the distortion obtained for the third and tenth pass. Even for the third pass (600 km), distortion is seen. The broadening rate vs. distance is plotted as in the previous cases as shown in Fig. 24. In this
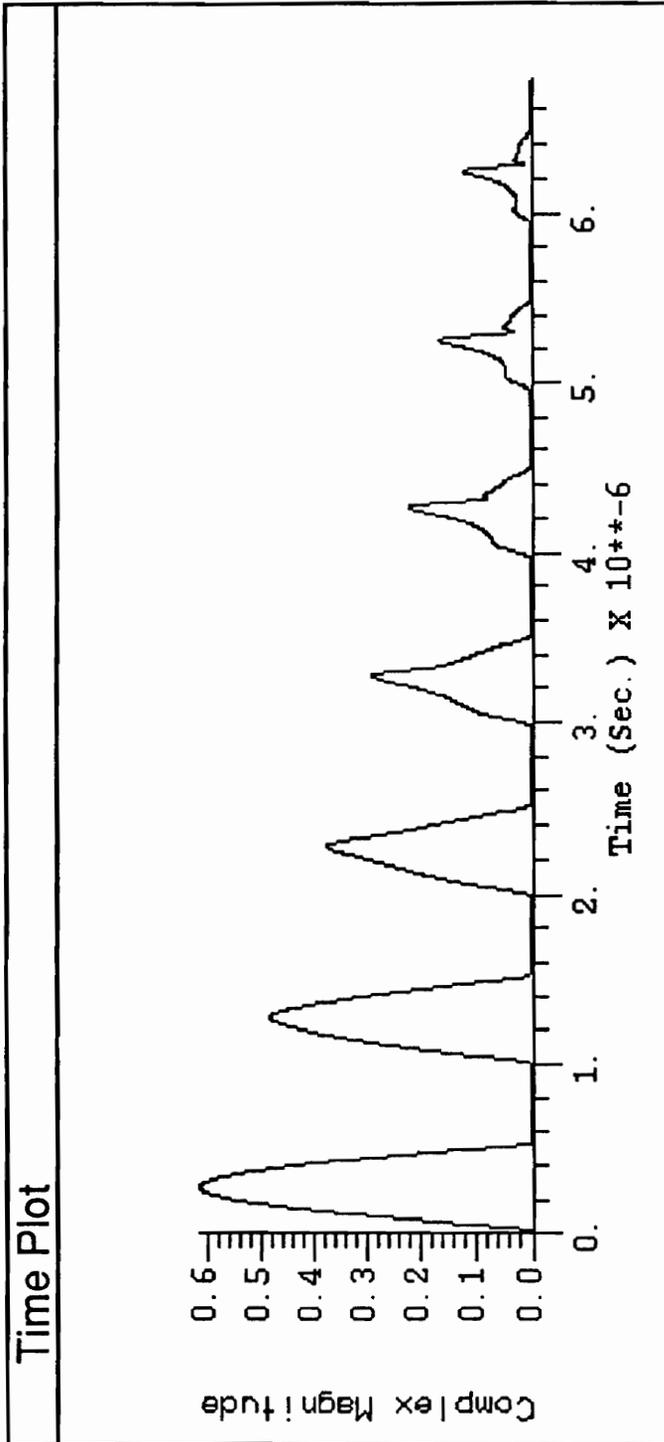
Figure 19 Ouput for case (3) - dispersion and nonlinearity, pass 1 to 7, pwr=5 mW
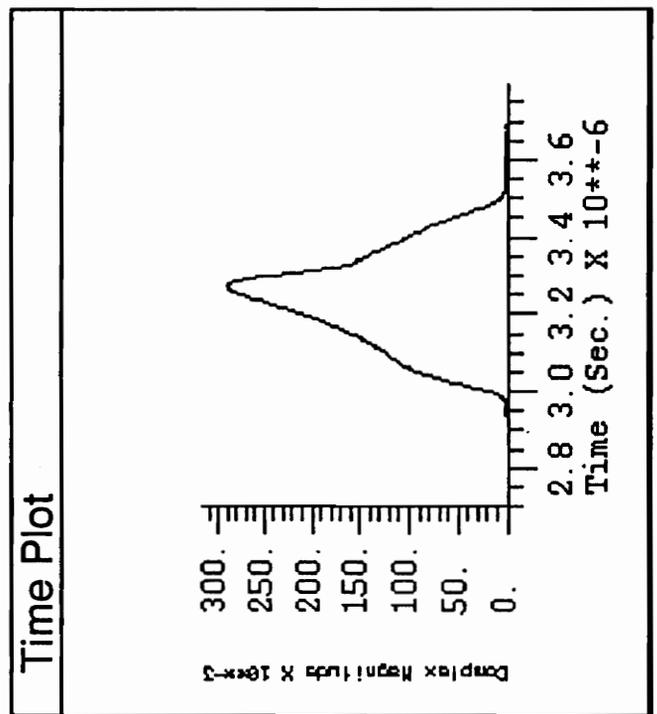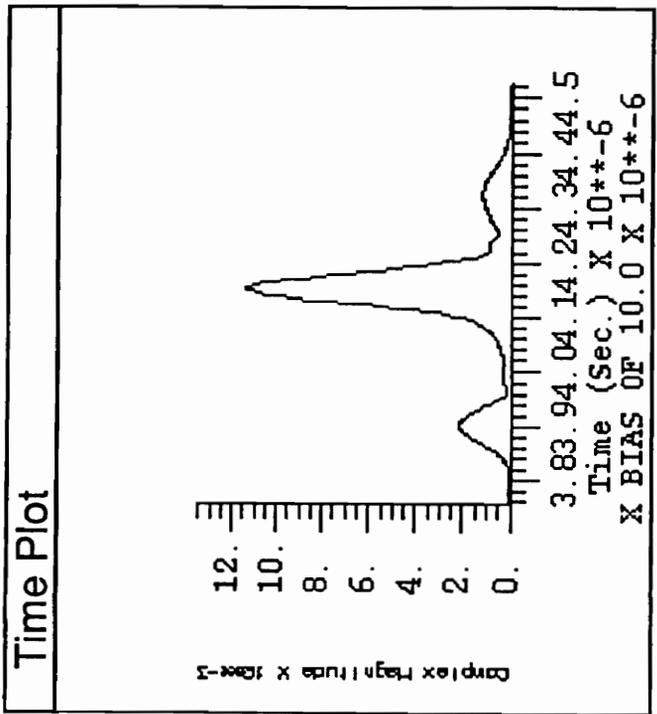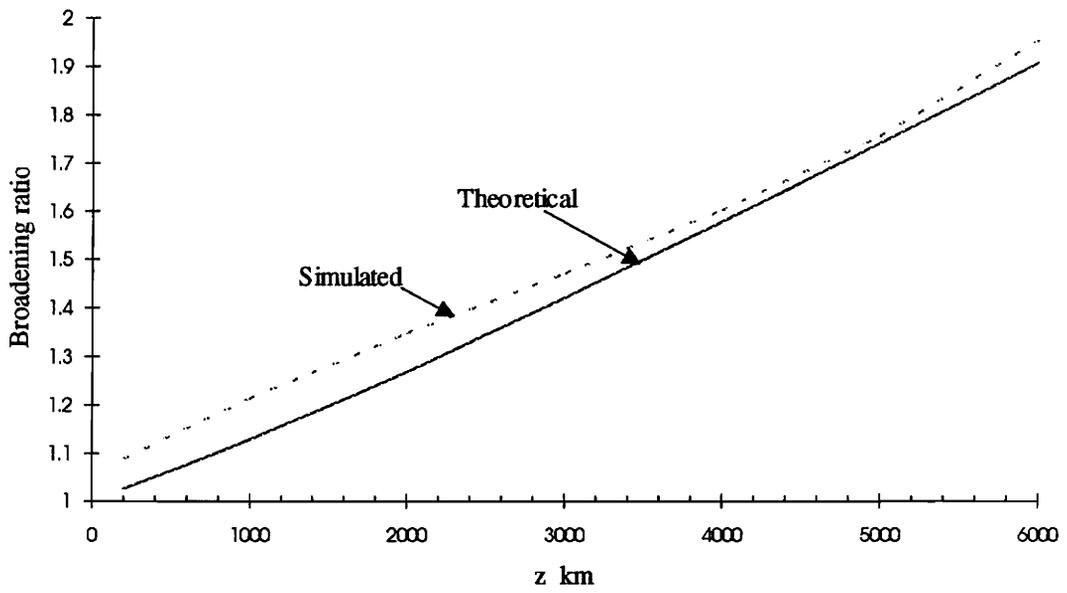
Figure 20. Output for case (3), for pass 4 and 15
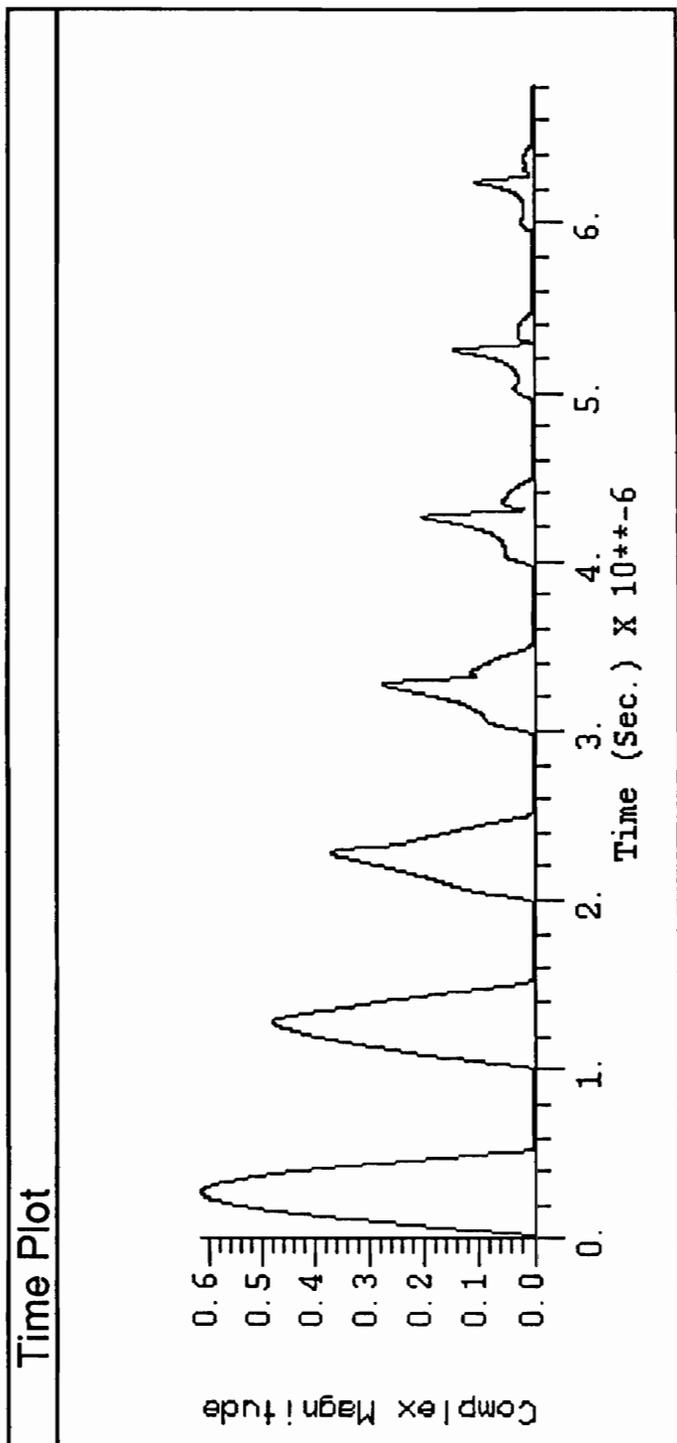
Figure 21. Broadening ratio vs. Distance for case (3)

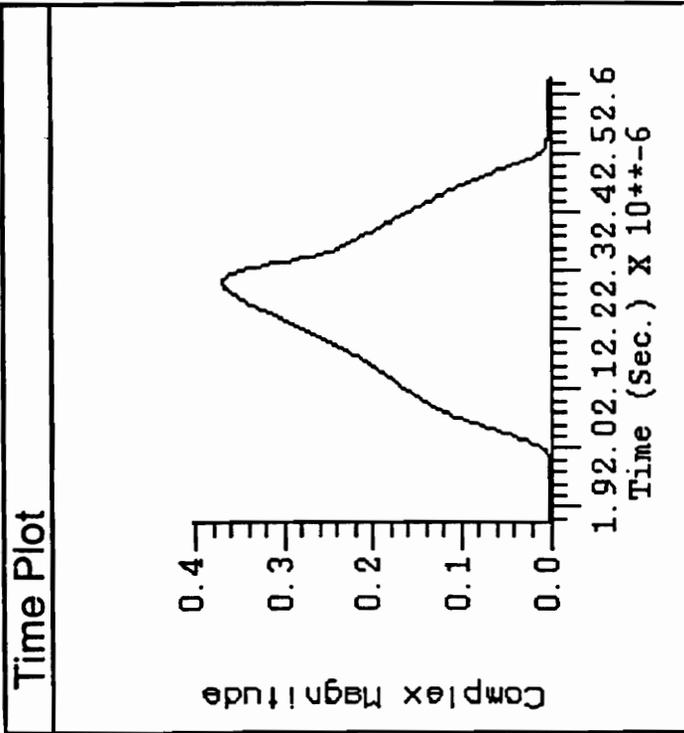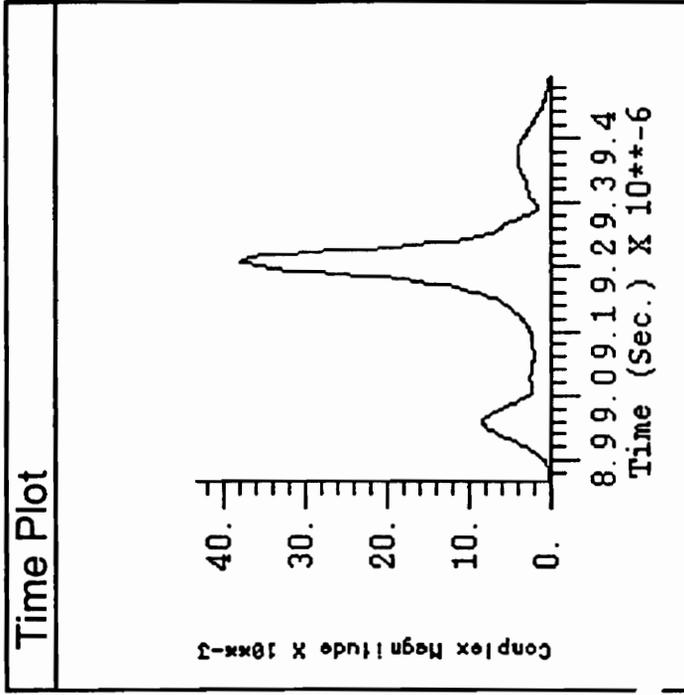Figure 22. Ouput for case (4) - dispersion and nonlinearity, pass 1 to 7, pwr=7 mW

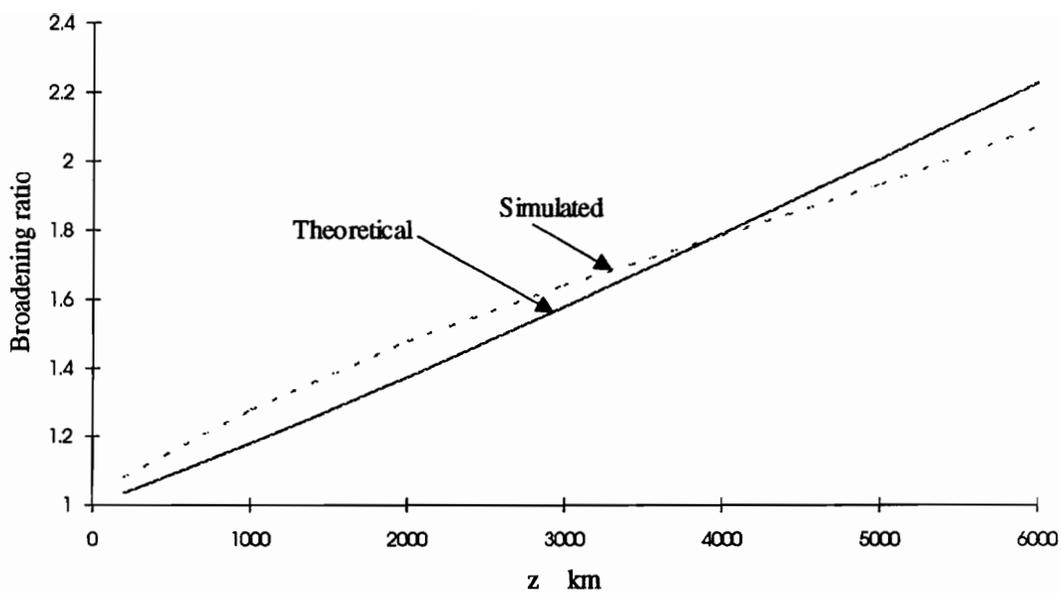Figure 23. Output for case (4), for pass 3 and 10

Figure 24. Broadening ratio vs. Distance for case (4)

graph it is seen that the broadening ratio decreases as compared to a Gaussian pulse after about 20 passes.

Comparing Figs. 18, 21 and 24 with the curve obtained for dispersion alone (Fig. 13), it is seen that SPM increases the broadening ratio as compared to when GVD occurs alone. The simulated and theoretical values show a similar characteristic. All measurements were taken by measuring the actual width of the pulse. A few readings were taken for each measurement and then the average was taken.

Case (5) D = -0.4 ps/km.nm, nonlinearity considered, power = 5 mW

We thought it would be interesting to see the effect of increasing the dispersion in the system. This would be the case in links of shorter distance where dispersion does not have to be kept low. D is taken to be -0.4 ps/km.nm, L_d is 915.5 km and power is 5 mW. To implement a system with higher dispersion, the value of $\beta_2 L$ of the filter must be higher. To achieve this a filter of higher order is required. A bandpass Butterworth filter of order 12 was used. Distortion comparable to case 3 and 4 is seen (Fig 25). The main point of interest in this case is the broadening ratio. Since dispersion is increased the broadening ratio should be larger than in case 3 where power is 5 mW but the dispersion is a magnitude lower than in this case. The pulse width was measured and a plot of broadening ratio vs. distance was plotted once again. The broadening ratio was indeed found to be larger than that in case 4 as seen in Fig. 26. However comparing the simulated results with the theoretical value for the Gaussian pulse (Fig. 27) it is seen that the broadening ratio obtained from the simulation increases by a much smaller extent than
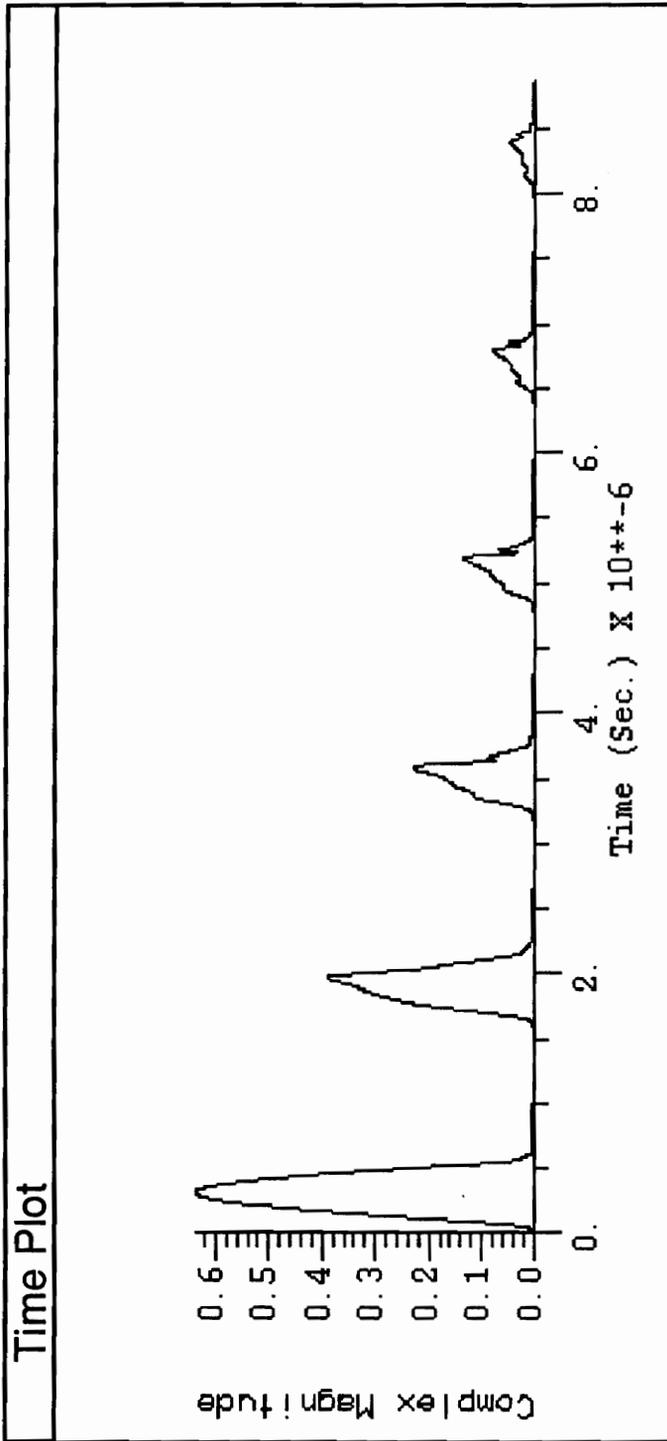
Figure 25. Output for case (5) - dispersion and nonlinearity, pass 1 to 6, pwr = 5 mW
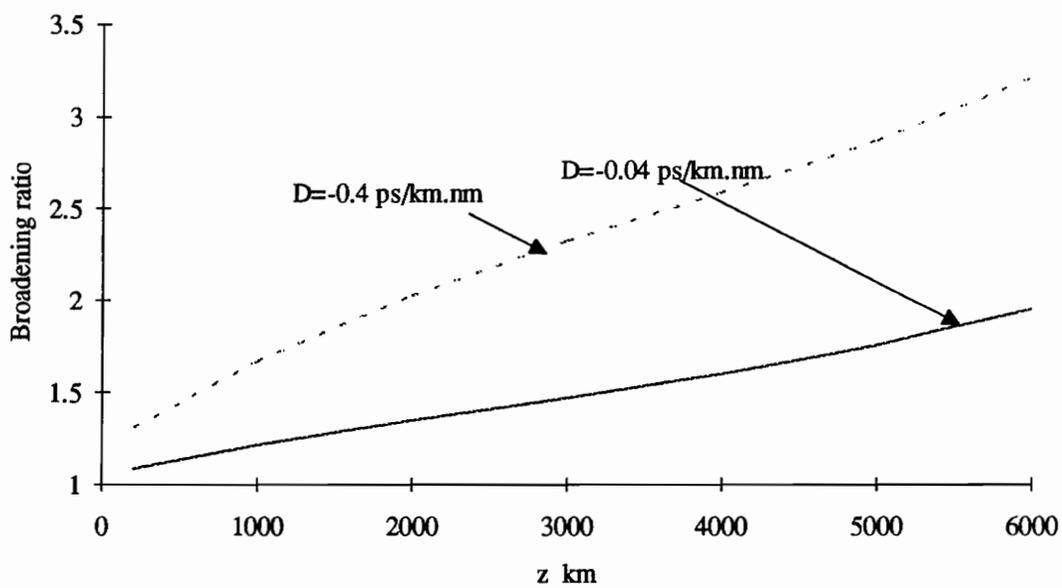
Figure 26. Broadening ratio vs. Distance for case (3) and case (5)
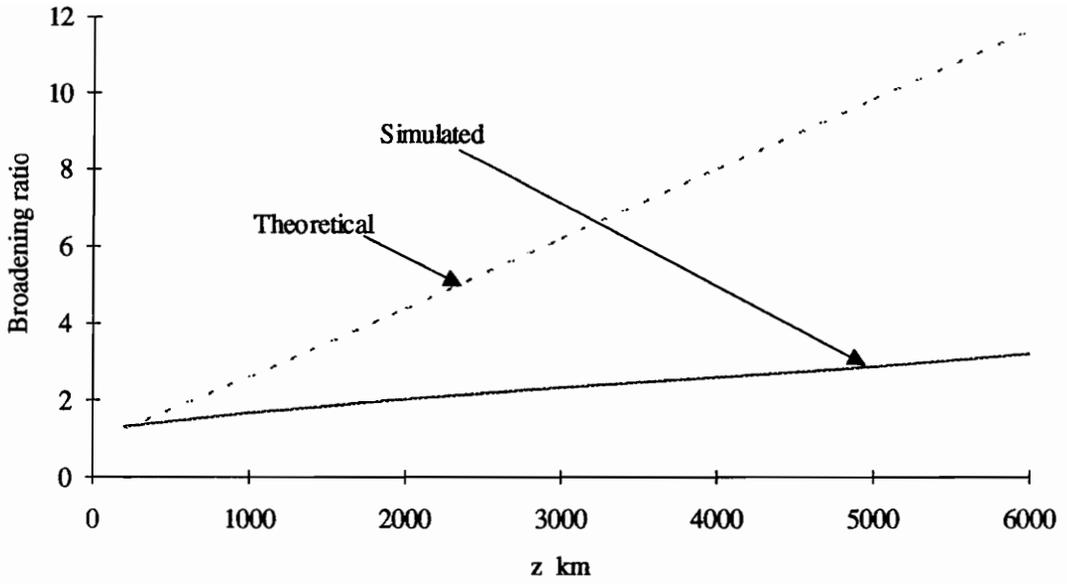
Figure 27. Broadening ratio vs. Distance for case (5)

the theoretical results. It was seen in case 1 that the effect of dispersion on a sinusoidal pulse causes a smaller amount of broadening as compared to the same effect on a Gaussian pulse. Since the effect of dispersion is more significant in this case than in the previous cases, the effect seen in case 1 may be the reason for the significant difference in simulated and theoretical values. Also, when the dispersion (phase distortion) is larger, there is also a larger amplitude distortion and this may be affecting the results. As discussed previously, when there is significant amplitude variation with frequency the spectral response narrows and consequently reduces dispersion.

4.3 Normalized parameters

There are two normalized parameters used in the circuit. They are $\dfrac{\beta_2 L}{(\text{bit period})^2}$ and $z_{\text{eff}}/L_{\text{nl}}$. Since $L_d = \dfrac{T_0^2}{|\beta_2|}$, the first parameter is essentially the ratio of the single pass length to the dispersion length, i.e.

$$\frac{\beta_2 L}{(\text{bit period})^2} = (\text{sgn } \beta_2)\frac{L}{L_d}. \tag{4.1}$$

It follows from eqn. (2.18) that

$$z_{\text{eff}} = \left(\frac{1 - e^{-\alpha z_{amp}}}{\alpha z_{amp}}\right) L. \tag{4.2}$$

For a 10 dB loss between amplifiers,

$$\frac{z_{\text{eff}}}{L_{nl}} = 0.5937 \frac{L}{L_{nl}}.$$

(4.3)

Therefore the second parameter is proportional to the ratio of the single pass length to the nonlinear length. Thus, the ratio of these two parameters is proportional to L_{nl}/L_d. Since the single pass length may be chosen arbitrarily (it is basically a step size in the integration), it is just the ratio of the two parameters (L_{nl}/L_d) that determines the normalized performance. Note that this also follows directly from eqn. (2.22). Therefore, there is no loss in generality in keeping one of the normalized parameters fixed and varying the other. For convenience, we chose to keep the dispersion parameter fixed and varied the nonlinearity factor, since this is easily done in the simulation by varying the VCO constant. To illustrate how the results may be scaled, we will consider a few examples

Consider the effect of increasing the coefficient of dispersion and thus β_2 by a factor of 10. To keep the value of $\dfrac{\beta_2 L}{(\text{bit period})^2}$ constant, the bit period is kept the same and the length of the fiber for one pass of the circuit is decreased by a factor of 10. In this case, dispersion has increased to -0.4 ps/km.nm and the fiber length for one pass becomes 20 km. Therefore to see the effect of nonlinearity for about 6000 km, many more iterations of the circuit must be taken.

Now consider the effect of decreasing the bit period of the fiber system by half, i.e. the bit

rate is now 5 Gb/s. To keep $\dfrac{\beta_2 L}{(\text{bit period})^2}$ constant once again, the length of one pass of

the circuit is increased to 800 km and the dispersion is kept constant. Therefore the

simulation results show that if the bit rate is decreased the same distortion will be seen

over a longer distance of the fiber link. Consequently if bit period is decreased by half but

the dispersion is increased by a factor of four, the same results will be obtained.

Therefore we see that the results obtained are not confined to a single case. Many

different combinations of parameters for a fiber system can be represented by using the

same simulation parameters.

Chapter 5: Conclusions and Further Work

5.1 Summary of results

With an increase in bit rate and power levels, the effects of nonlinearity have become of concern. The various nonlinear effects were outlined in chapter 2 and although they are generally harmful effects, they can also be used to an advantage. For example, they can be used in obtaining optical pulse compression, in compensating for dispersion and in soliton pulse transmission. In the area of communications, nonlinear couplers, optical switches and modulators based on these effects have been implemented and used [9].

Chapter 2 outlined the theory of SPM and GVD and it's combined effect. The circuit modeling GVD and the SPM nonlinearity was designed to consist of readily available components and yet have flexibility in setting determining parameters such as filter bandwidth, bit rate, VCO free-running frequency etc. The bandpass Butterworth filter modeled dispersion adequately for up to about 10 passes of the circuit (2000 km). For long distance links having dispersion close to the zero dispersion wavelength (ZDWL), it was found that the effect of nonlinearity overpowers the effect of dispersion and

considerable broadening of the pulse takes place. This limits the bandwidth of the fiber system. The circuit was seen to behave as expected. The input pulse distorts due to SPM and breaks up into peaks. This effect is more prominent as input power increases. SPM enhances the broadening of the pulse as compared to GVD alone. The broadening ratio for a Gaussian and sinusoidal pulse exhibit the same behavior but are different in value. Thus we conclude that the amount of broadening in a pulse depends on its shape. The significance of using normalized parameters in the circuit model was discussed in section 4.3, where it was shown that the results may be scaled to apply to a large range of cases.

Thus an electrical circuit was designed and simulated to model a nonlinear, dispersive long distance links. We see that without having to use elaborate apparatus and an experimental set-up, we were able to show the effects of GVD and SPM nonlinearity in a pulse and observe the outcome.

5.2 Further work

Apart from physically implementing the circuit, there are many other enhancements that can be made to the circuit and simulation using BOSS.

• A noise model could be designed and introduced into the circuit to see the effect of noise with nonlinearity. Various types of noise could be incorporated such as ASE noise in optical amplifiers, shot noise, thermal noise or Gaussian noise.

- Various equalization and compensation techniques can be studied.

- The effect of solitons and pulse compression could be simulated. To obtain solitons, the self chirping and dispersion must act in the proper direction and have the proper magnitudes for pulse compression to exactly cancel the tendency of dispersion to broaden the pulse [1].

- The effect of inter-symbol interference (ISI) between consecutive pulses could be studied by altering the time delay between consecutive pulses.

- Since results seem to be sensitive to pulse shape, the effect of different input pulse shapes could be evaluated.

- The effect of optical filtering could be simulated.

References

[1]   S. E. Miller and I. P. Kaminov, 'Optical fiber telecommunications II,' Academic Press Inc., 1988, pp. 56-107.

[2]   Trudy Bell, 'Telecommunications,' IEEE Spectrum, Jan. 1992, pp. 36-38.

[3]   A. R. Chraplyvy, 'Limitations on lightwave communications imposed by optical-fiber nonlinearities,' Journal of Lightwave Tech, vol. 8, no. 10, Oct. 1990, pp. 1548-1551.

[4]   Govind P. Agrawal 'Nonlinear Fiber Optics', Boston, Academic Press Inc., 1989.

[5]   G. Veith, 'Self-phase modulation in optical fibers,' SPIE, vol. 864 Advanced Opto. Tech., 1987, pp. 154-161.

[6]   L. F. Mollenaur, M. J. Neubelt, et al, 'Experimental study of soliton transmission over more than 10,000 km in dispersion-shifted fiber,' Optic Letters, vol. 15, No. 21, Nov. 1990, pp. 1203-1205.

[7]   K. Sam Shanmugan, 'An update on software packages for simulation of communication systems (links),' IEEE Journal on Selected Areas in Communications, vol. 6, no.1, Jan. 1988, pp. 10-11.

[8]   R. H. Stolen and C. Lin, 'Self-phase modulation in silica optical fibers', Physics review A, vol. 17, No. 4, April 1978, pp. 1448-1453.

[9]   D. Cotter, 'Fibre nonlinearities in optical communications', Optical and Quantum Electronics 19, 1987, pp. 1-17.

[10]   Hermann A. Haus, 'Molding light into solitons', IEEE Spectrum, March 1993, pp. 48-53.

Vita

Shilpa D. Mehta was born on November 9, 1968 in Bryn Mawr, PA. At the age of ten she moved to Bombay, India with her parents. She received her Bachelor of Engineering (Electronics) degree from Thadomal Shahani Engineering College, Bombay University in May 1991. To pursue a higher education in digital and optical communications, she then returned to the country of her birth. She enrolled in the master's program at the Bradley Department of Electrical and Computer Engineering, Virginia Polytechnic Institute and State University. She obtained a research assistantship under her advisor Dr. Ira Jacobs. She received her Master's degree in July 1993.